

Table 3 Correlation between surgical cytoreduction and peritoneal cytology at IS ($n = 50$)

IS	Peritoneal cytology at IS	
	Negative	Positive
Complete ($n = 32$)	23	9
Incomplete ($n = 18$)	5	13
Total	28	22

Fisher's exact test, $P = 0.0035$. IS, interval surgery.

Identification of significant prognostic factors detected at IS

As shown in Figure 1, median PFS and OS for all cases were 14.8 and 50.7 months, respectively. The corresponding 3-year PFS and OS for all cases were 13.1% and 64.5%, respectively.

The impact of various clinicopathological factors for poor PFS prognosis was examined by univariate and multivariate analysis. On univariate analysis, we investigated the prognostic significance of the following factors: age (≥ 60 years), histologic type (clear cell, mucinous, low-grade serous vs endometrioid, high-grade serous), primary treatment (NAC, PDS), preoperative serum CA-125 levels (titer, ≥ 20 U/mL), response of pre-IS chemotherapy (cCR, non-cCR), maximum diameter of largest residual tumor nodule detected at IS (≥ 1 cm), number of residual lesions at IS (number ≥ 20), peritoneal cytology positivity, and surgical completeness (postoperative presence of residual lesions). As shown in Table 4, univariate analysis revealed that preoperative serum CA-125 level (relative risk [RR] = 1.060, 95% confidence interval [CI] = 0.568–1.960, $P = 0.0539$), number of residual lesions at secondary surgery (< 20 , RR = 1.838, 95% CI = 0.936–3.502, $P = 0.0554$ by log-rank test), positive peritoneal cytology (RR = 2.851, 95% CI = 1.437–5.821, $P = 0.0015$ by log-rank test) and surgical completeness (RR = 2.103, 95% CI = 1.089–4.005, $P = 0.0171$ by log-rank test) were significant for PFS. Multivariate analysis (Table 5) revealed that positive peritoneal cytology (RR = 2.355, 95% CI = 1.084–5.285, $P = 0.0303$ by log-rank test) was the only independent poor prognostic factor for PFS.

OS and PFS by prognostic factors at IS

Overall survival and PFS survival curves in our cases were assessed for representative prognostic factors using the Kaplan–Meier method and the log-rank test. Complete cytoreduction cases at IS demonstrated significantly better prognosis for both OS and PFS than cases with incomplete surgery (OS, $P < 0.0001$; PFS,

$P = 0.017$ by log-rank test) (Fig. 2). We also observed a significant difference in both OS and PFS between peritoneal cytology-negative and -positive cases (OS, $P < 0.0001$; PFS, $P = 0.0015$ by log-rank test) (Fig. 3). Cytology-negative cases showed good prognosis even in those with T3c disease, including a 3-year OS rate of 78% and median PFS of 18 months. Notably, nine of 32 cases with complete cytoreduction were cytology-positive. Among these nine cases, all eventually experienced disease recurrence. Two of the nine survived with recurrent diseases, while six patients died, likely due to the chemoresistant status of disease. There was no significant difference in OS and PFS by Kaplan–Meier method in terms of amount of residual tumor and serum CA-125 level, even though these factors showed marginal significance on univariate analysis (survival curves not shown).

Discussion

The role of IS was first shown by Berek *et al.* as a suitable option to prolong survival after incomplete primary treatment.²² It remained controversial for several decades thereafter whether NAC or PDS, followed by IS, provided additional benefit compared with standard treatment without IS.^{10,12,23} However, it was subsequently shown that NAC, followed by appropriate interval cytoreduction, could indeed improve survival in those with unresectable gross tumors involving multiple intra-abdominal organs in whom primary surgery was suboptimal due to low PS. It was additionally suggested that this approach may result in lower perioperative complication rates compared with standard initial aggressive resection.^{16,21,24} Although the goal of the interval surgery is to have minimal residual disease remaining at the completion of the operative procedure, the determination of optimal cytoreduction and postoperative therapy regimens are primarily determined by intraoperative surgical evaluation through subjective visualization and palpation. Thus, a validated documentation system, Intraoperative Mapping of Ovarian Cancer (IMO), has been proposed as an informative guideline for evaluation.²⁵ However, though a validated documentation system exists for identifying and recording tumor dissemination pattern and postoperative tumor residuals, discordant results are not uncommon after intraoperative assessment.^{26,27} In contrast, peritoneal cytology, with a sensitivity and specificity of approximately 66% and 100%, respectively, is usually performed as a subsidiary measurement in conjunction with direct

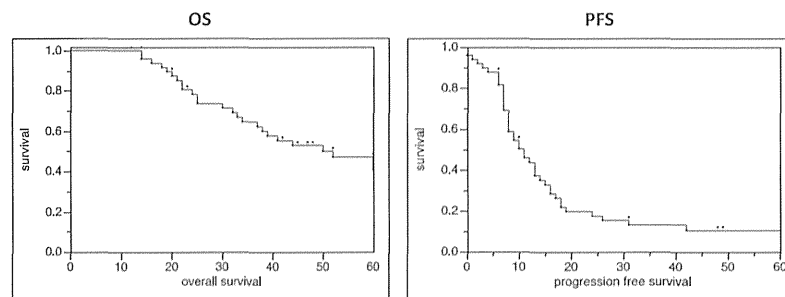


Figure 1 Overall survival (OS) and progression-free survival (PFS) of all stage T3c ovarian cancer patients ($n = 50$). The median PFS and OS for all cases in the study were 14.8 and 50.7 months, respectively. The corresponding 3-year PFS and OS for all cases in the study were 64.5% and 13.1%, respectively.

Table 4 Univariate analysis for PFS

	RR	95% CI	P
Age (≥ 60 vs < 60 years)	1.230	0.668–2.277	0.4907
Histology (CC + M + LGS vs HGS + E)	0.710	0.169–2.006	0.5563
Pretreatment of IS (NAC vs PDS + chemotherapy)	1.058	0.529–2.004	0.8621
CA-125 at IS (≥ 20 vs < 20 IU/mL)	1.060	0.568–1.960	0.0539
Response of pre-IS chemotherapy (cCR vs non-cCR)	1.078	0.586–1.997	0.8019
Maximum size of residual tumor (≥ 1 cm vs < 1 cm)	1.604	0.859–3.008	0.1210
No. of residual tumors at IS (≥ 20 vs < 20)	1.838	0.936–3.502	0.0554
Peritoneal cytology at IS (positive vs negative)	2.851	1.437–5.821	0.0015
Any residual tumor after IS (complete vs incomplete)	2.103	1.089–4.005	0.0171

Bolding indicates statistical significance. CA, cancer antigen; CC, clear cell carcinoma; CI, confidence interval; cCR, clinical complete response; E, endometrioid carcinoma; HGS, high-grade serous carcinoma; IS, interval surgery; LGS, low-grade serous carcinoma; M, mucinous cell carcinoma; NAC, neoadjuvant chemotherapy; PDS, primary debulking surgery; PFS, progression-free survival; RR, relative risk.

Table 5 Multivariate analysis for PFS

	RR	95% CI	P
CA-125 at IS (≥ 20 vs < 20 U/mL)	1.172	0.418–1.744	0.6625
No. of residual tumor at IS (≥ 20 vs < 20)	1.261	0.511–3.053	0.6122
Any residual tumor after IS (complete vs incomplete)	1.218	0.487–3.079	0.6750
Peritoneal cytology at IS (positive vs negative)	2.355	1.084–5.285	0.0303

Bolding indicates statistical significance. CA, cancer antigen; CI, confidence interval; IS, interval surgery; PFS, progression-free survival; RR, relative risk.

visualization,²⁸ confirming the presence of peritoneal implants with few clinical biases. Further the intensively wiped peritoneal swabs were additionally assessed for the cytological evaluation of the peritoneal cavity in our institute.

Although it may be necessary to investigate more cases to draw a definite conclusion, it raises useful suggestions of the significance of intraoperative diagnostic evaluation. Our study demonstrates diagnostic value for predicting outcome of stage T3c ovarian cancer patients at IS and shows that the presence of positive peritoneal cytology at IS is an independent adverse prognostic variable with regard to PFS on both multivariate and survival analyses. In terms of diagnos-

tic significance, peritoneal cytology at IS may be a very useful tool for predicting prognosis of T3c cases. Moreover, our data suggested that negative peritoneal cytology was more strongly associated with favorable prognosis compared with complete cytoreduction. Thus, cytology-negative cases showed good prognosis even in those with T3c disease, including a 3-year OS rate of more than 60% and median PFS of 18 months. In comparison, median PFS in EORTC trial cases was 12 months.

Notably, nine of 32 cases with complete cytoreduction were cytology-positive, suggesting that residual cancer cells, possibly chemoresistant, remained microscopically present in the peritoneum.

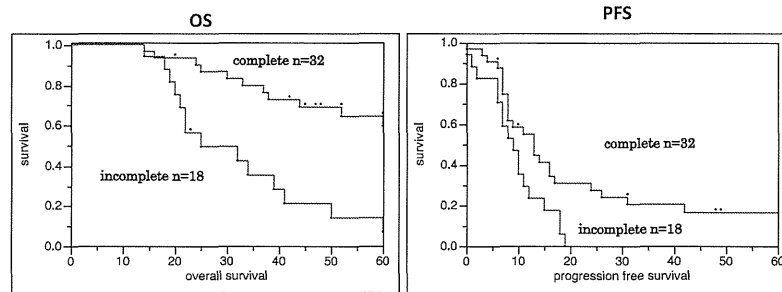


Figure 2 Impact of surgical reduction rate at interval surgery (IS): complete versus incomplete ($n = 50$). Three-year overall survival (OS) for complete cytoreduction cases in the study was 79%, and for incomplete cases was 13.1%. Complete cytoreduction cases at IS have better prognosis for both OS and progression-free survival (PFS) significantly than cases that ended as incomplete surgery (OS, $P < 0.0001$; PFS, $P = 0.017$ by log-rank test).

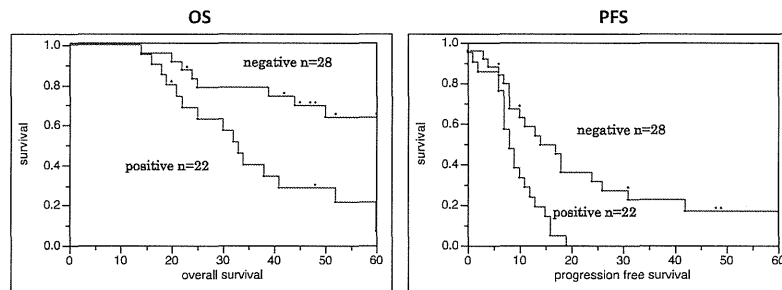


Figure 3 Comparison of peritoneal cytology at interval surgery (IS): positive versus negative ($n = 50$). A significant difference in both overall survival (OS) and progression-free survival (PFS) between the peritoneal cytology-negative and -positive (OS, $P < 0.0001$; PFS, $P = 0.0015$ by log-rank test) is shown. Cytology-negative cases show good prognosis even for T3c cases; 3-year OS rate of 78% and median PFS of 18 months.

Among these nine cases, all eventually experienced disease recurrence. Peritoneal cytology may be more sensitive for detection of residual cancer cells at IS compared with intraoperative surgical evaluation via visualization and palpation, or CT scanning. Microscopic residual cancer cells may progress to recurrent tumor even after additional post-IS adjuvant chemotherapy, followed by clinical recurrence. Our data suggests that peritoneal cytology should be assessed at IS in order to identify T3c cases with poor prognosis, most of which develop intraperitoneal recurrence.

Given our data, peritoneal cytology at IS provides us with additional information with which to predict PFS in individual cases, as well as reconsider post-IS adjuvant chemotherapy regimens for cytology-positive cases. Recent reports from Japan have demonstrated that i.p., versus i.v., administration of chemotherapy was more effective in ovarian cancer cases in which IDS ended with suboptimal surgery (KCOG9812).²⁹ Cytology-positive cases may warrant either change of

regimen or route of administration for post-IS adjuvant chemotherapy. Obviously, randomized well-designed prospective studies are warranted to investigate new strategies for post-IS adjuvant chemotherapy in peritoneal cytology-positive cases.

Acknowledgments

The authors are grateful to Dr Gautam A. Deshpande (St Luke's International Hospital, John A. Burns School of Medicine) for the critical reading of our manuscript. This work was supported by a Grant-in-Aid for Scientific Research (K. K.) from the Ministry of Education, Science and Culture, Japan.

Disclosure

None declared.

References

1. Ferlay J, Shin HR, Bray F, Forman D, Mathers C, Parkin DM. Estimates of worldwide burden of cancer in 2008: GLOBOCAN 2008. *Int J Cancer* 2010; **127**: 2893–2917.
2. Sankaranarayanan R, Ferlay J. Worldwide burden of gynaecological cancer: The size of the problem. *Best Pract Res Clin Obstet Gynaecol* 2006; **20**: 207–225.
3. Jemal A, Bray F, Ferlay J. Global cancer statistics. *CA Cancer J Clin* 2011; **61**: 69–90.
4. Ushijima K. Current status of gynecologic cancer in Japan. *J Gynecol Oncol* 2009; **20**: 67–71.
5. Bristow RE, Tomacruz RS, Armstrong DK, Trimble EL, Montz FJ. Survival effect of maximal cytoreductive surgery for advanced ovarian carcinoma during the platinum era: A meta-analysis. *J Clin Oncol* 2002; **20**: 1248–1259.
6. Fanfani F, Ferrandina G, Corrado G *et al.* Impact of interval debulking surgery on clinical outcome in primary unresectable FIGO stage IIIC ovarian cancer patients. *Oncology* 2003; **65**: 316–322.
7. Winter WE, Maxwell GL, Tian C *et al.* Prognostic factors for stage III epithelial ovarian cancer: A Gynecologic Oncology Group Study. *J Clin Oncol* 2007; **25**: 3621–3627.
8. Weinberg LE, Rodriguez G, Hurteau JA. The role of neoadjuvant chemotherapy in treating advanced epithelial ovarian cancer. *J Surg Oncol* 2010; **101**: 334–343.
9. Bonnefoi H, A'Hern RP, Fisher C *et al.* Natural history of stage IV epithelial ovarian cancer. *J Clin Oncol* 1999; **17**: 767–775.
10. Rauh-Hain JA, Winograd D, Growdon WB *et al.* Prognostic determinants in patients with uterine and ovarian clear carcinoma. *Gynecol Oncol* 2012; **125**: 376–380.
11. van der Burg ME, van Lent M *et al.* The effect of debulking surgery after induction chemotherapy on the prognosis in advanced epithelial ovarian cancer. Gynecological Cancer Cooperative Group of the European Organization for Research and Treatment of Cancer. *N Engl J Med* 1995; **332**: 629–634.
12. Rose PG, Nerenstone S, Brady MF *et al.* Secondary surgical cytoreduction for advanced ovarian carcinoma. *N Engl J Med* 2004; **351**: 2489–2497.
13. Tangitgamol S, Manusirivithaya S, Laopaiboon M *et al.* Interval debulking surgery for advanced epithelial ovarian cancer: A Cochrane systematic review. *Gynecol Oncol* 2009; **112**: 257–264.
14. Onda T, Yoshikawa H. Neoadjuvant chemotherapy for advanced ovarian cancer: Overview of outcomes and unanswered questions. *Expert Rev Anticancer Ther* 2011; **11**: 1053–1067.
15. Chang S-J, Bristow RE, Ryu H-S. Impact of complete cytoreduction leaving no gross residual disease associated with radical cytoreductive surgical procedures on survival in advanced ovarian cancer. *Ann Surg Oncol* 2012; **19**: 4059–4067.
16. Vergote I, Tropé CG, Amant F *et al.* Neoadjuvant chemotherapy or primary surgery in stage IIIC or IV ovarian cancer. *N Engl J Med* 2010; **363**: 943–953.
17. Dewdney SB, Rimel BJ, Reinhart AJ *et al.* The role of neoadjuvant chemotherapy in the management of patients with advanced stage ovarian cancer: Survey results from members of the Society of Gynecologic Oncologists. *Gynecol Oncol* 2010; **119**: 18–21.
18. Vergote I, Amant F, Kristensen G *et al.* Primary surgery or neoadjuvant chemotherapy followed by interval debulking surgery in advanced ovarian cancer. *Eur J Cancer* 2011; **47** (Suppl 3): S88–S92.
19. du Bois A, Marth C, Pfisterer J *et al.* Neoadjuvant chemotherapy cannot be regarded as adequate routine therapy strategy of advanced ovarian cancer. *Int J Gynecol Cancer* 2012; **22**: 182–185.
20. Le T, Alshaikh G, Hopkins L *et al.* Prognostic significance of postoperative morbidities in patients with advanced epithelial ovarian cancer treated with neoadjuvant chemotherapy and delayed primary surgical debulking. *Ann Surg Oncol* 2006; **13**: 1711–1716.
21. Onda T, Yoshikawa H, Yasugi T *et al.* The optimal debulking after neoadjuvant chemotherapy in ovarian cancer: Proposal based on interval look during upfront surgery setting treatment. *Jpn J Clin Oncol* 2010; **40**: 36–41.
22. Berek JS, Hacker NF, Lagasse LD *et al.* Survival of patients following secondary cytoreductive surgery in ovarian cancer. *Obstet Gynecol* 1983; **61**: 189–193.
23. Redman CW, Warwick J, Luesley DM *et al.* Intervention debulking surgery in advanced epithelial ovarian cancer. *Br J Obstet Gynaecol* 1994; **101**: 142–146.
24. Morice P, Rey A, Atallah D *et al.* Results of interval debulking surgery in advanced stage ovarian cancer?: An exposed – Non-exposed study. *Ann Oncol* 2003; **14**: 74–77.
25. Sehouli J, Savvatis K, Braicu E-I *et al.* Primary versus interval debulking surgery in advanced ovarian cancer: Results from a systematic single-center analysis. *Int J Gynecol Cancer* 2010; **20**: 1331–1340.
26. Chi DS, Barlin JN, Ramirez PT *et al.* Follow-up study of the correlation between postoperative computed tomographic scan and primary surgeon assessment in patients with advanced ovarian, tubal, or peritoneal carcinoma reported to have undergone primary surgical cytoreduction to residual disease. *Int J Gynecol Cancer* 2010; **20**: 353–357.
27. Rose PG, Brady MF. Gynecologic oncology EORTC 55971?: Does it apply to all patients with advanced state ovarian cancer?? *Gynecol Oncol* 2011; **120**: 300–301.
28. Karoo ROS, Lloyd TDR, Garcea G *et al.* How valuable is ascitic cytology in the detection and management of malignancy? *Postgrad Med J* 2003; **79**: 292–294.
29. Tsubamoto H, Itani Y, Ito K *et al.* Phase II study of interval debulking surgery followed by intraperitoneal chemotherapy for advanced ovarian cancer: A Kansai Clinical Oncology Group study (KCOG9812). *Gynecol Oncol* 2013; **128**: 22–27.

Human Papillomavirus Genotype Distribution in Cervical Intraepithelial Neoplasia Grade 2/3 and Invasive Cervical Cancer in Japanese Women

Yukari Azuma¹, Rika Kusumoto-Matsuo¹, Fumihiko Takeuchi¹, Asami Uenoyama², Kazunari Kondo², Hajime Tsunoda², Kazunori Nagasaka³, Kei Kawana³, Tohru Morisada⁴, Takashi Iwata⁴, Daisuke Aoki⁴ and Iwao Kukimoto^{1,*}

¹WHO HPV LabNet Regional Reference Laboratory, WHO Western Pacific Region, Pathogen Genomics Center, National Institute of Infectious Diseases, Tokyo, ²Department of Obstetrics and Gynecology, NTT Medical Center Tokyo, Tokyo, ³Department of Obstetrics and Gynecology, Graduate School of Medicine, The University of Tokyo, Tokyo and ⁴Department of Obstetrics and Gynecology, Keio University School of Medicine, Tokyo, Japan

*For reprints and all correspondence: I. Kukimoto, Pathogen Genomics Center, National Institute of Infectious Diseases, 4-7-1 Gakuen, Musashi-murayama, Tokyo 208-0011, Japan. E-mail: ikuki@nih.go.jp

Received 22 May 2014; accepted 18 July 2014

Objective: Human papillomavirus vaccines are being introduced worldwide and are expected to reduce the incidence of cervical cancer. Here we report a cross-sectional study using a validated human papillomavirus genotyping method to reveal the human papillomavirus prevalence and genotype distribution in Japanese women with cervical intraepithelial neoplasia Grade 2/3 and invasive cervical cancer.

Methods: Cervical exfoliated cells were collected from 647 patients with abnormal cervical histology (cervical intraepithelial neoplasia Grade 2, $n = 164$; cervical intraepithelial neoplasia Grade 3, $n = 334$; and invasive cervical cancer, $n = 149$), and subjected to the PGMY-PCR-based genotyping assay. The association between human papillomavirus infection and lesion severity was calculated using a prevalence ratio.

Results: Overall, the prevalence of human papillomavirus deoxyribonucleic acid was 96.3% in cervical intraepithelial neoplasia Grade 2, 98.8% in cervical intraepithelial neoplasia Grade 3 and 88.0% in invasive cervical cancer (97.8% in squamous cell carcinoma and 71.4% in adenocarcinoma). The three most prevalent types were as follows: human papillomavirus 16 (29.3%), human papillomavirus 52 (27.4%) and human papillomavirus 58 (22.0%) in cervical intraepithelial neoplasia Grade 2; human papillomavirus 16 (44.9%), human papillomavirus 52 (26.0%) and human papillomavirus 58 (17.4%) in cervical intraepithelial neoplasia Grade 3; and human papillomavirus 16 (47.7%), human papillomavirus 18 (23.5%) and human papillomavirus 52 (8.7%) in invasive cervical cancer. The prevalence ratio of human papillomavirus 16 was significantly higher in cervical intraepithelial neoplasia Grade 3 compared with cervical intraepithelial neoplasia Grade 2 (prevalence ratio, 1.62; 95% confidence interval, 1.26–2.13) and in squamous cell carcinoma compared with cervical intraepithelial neoplasia Grade 3 (prevalence ratio, 1.55; 95% confidence interval, 1.25–1.87). Multiple infections decreased from cervical intraepithelial neoplasia Grade 2/3 (38.4/29.6%) to invasive cervical cancer (14.1%), whereas co-infections with human papillomavirus 16/52/58 were found in cervical intraepithelial neoplasia Grade 2/3.

Conclusions: The results of this study provide pre-vaccination era baseline data on human papillomavirus type distribution in Japanese women and serve as a reliable basis for monitoring the future impact of human papillomavirus vaccination in Japan.

Key words: human papillomavirus – genotyping – cervical cancer – prevalence ratio

INTRODUCTION

Persistent infection with a subset of human papillomaviruses (HPVs), known as high-risk HPVs, is a primary cause of the development of cervical precancerous lesions and invasive cervical cancer (ICC) (1). At least 15 genotypes (HPV16, 18, 31, 33, 35, 39, 45, 51, 52, 56, 58, 59, 68, 73 and 82) are recognized as high-risk HPVs (2), among which HPV16 is most frequently detected in ICC cases worldwide, followed by HPV18. Recent worldwide introduction of HPV vaccines targeting HPV16/18 (Cervarix[®] and Gardasil[®]) is expected to prevent incident HPV16/18 infection, thereby reducing cervical cancer cases (3). However, clinical trials on HPV vaccines have so far only evaluated its efficacy in preventing precancerous lesions, including cervical intraepithelial neoplasia (CIN) Grades 2 and 3, as a surrogate clinical endpoint, and its final effect on reducing ICC cases is not yet proven. Because the progression into ICC generally requires >10 years of persistent HPV infection, HPV type distribution in CIN2/3 lesions in the general population provides an early indicator to assess the effectiveness of HPV vaccination and thus to estimate any subsequent reduction in ICC cases.

East Asian countries including China, Korea and Japan show region-specific variation in HPV type distribution in ICC cases (4). In particular, HPV52 and HPV58 are more prevalent in these countries compared with Europe, North America and Africa (5, 6). Previous studies report that HPV16/18 cause the majority of ICC cases in Japan (7–10), ranging from 50 to 70%, whereas HPV52/58 are individually detected in ~7% of Japanese ICC cases. Since the HPV vaccines against HPV16/18 infection have exhibited only a limited efficacy for cross protection against other high-risk HPVs (11) it is important to monitor the prevalence of HPV52/58 in CIN2/3 and ICC cases in order to evaluate whether type-replacement occurs in post-vaccination era Japan.

In this study, we used a validated HPV genotyping method (12) to record the most recent data on the prevalence and type distribution of high-risk HPVs in Japanese women with CIN2/3 lesions and ICC. The results provide reliable baseline data on the HPV type distribution in Japanese women with precancerous lesions and cervical cancer that will enable accurate assessment of any future impact from HPV vaccination in Japan.

PATIENTS AND METHODS

STUDY SUBJECTS AND SPECIMEN COLLECTION

We enrolled 647 Japanese women who were histologically diagnosed with CIN2/3 or ICC by punch biopsy or cervical conization (CIN2, $n = 164$; CIN3, $n = 334$; and ICC, $n = 149$) at three hospitals in the Tokyo metropolitan area (NTT Medical Center Tokyo, Keio University Hospital, and The University of Tokyo Hospital) from September 2009 to December 2013. Histological diagnosis was made using hematoxylin–eosin-stained sections according to the World Health Organization (WHO) classification by experienced

pathologists at each hospital. When diagnoses between punch biopsy and cervical conization were discordant, a higher grade of histology was taken as final diagnosis. The mean age \pm standard deviation and age range in each histological grade was as follows: CIN2, 36.4 ± 7.7 years (21–62 years); CIN3, 38.9 ± 8.0 years (21–67 years); ICC, 48.0 ± 14.9 years (27–88 years). In Japan, Cervarix[®] and Gardasil[®] were approved for use in 2009 and 2011, respectively, but all the study participants reported no history of HPV vaccination except for one CIN2 case that had recently been administered with Gardasil[®].

Before histopathological diagnosis, cervical exfoliated cells were collected in Thinprep[®] media using a Cervex-brush[®] combi for subsequent HPV genotyping. The study protocol was approved by the Ethics Committee at each hospital and the National Institute of Infectious Diseases, and written informed consent for study participation was obtained from each patient.

HPV GENOTYPING

DNA extraction and HPV genotyping were centralized in a laboratory at the National Institute of Infectious Diseases. Total DNA was extracted from a 200- μ l aliquot of cervical exfoliated cells using the QIAamp DNA Blood Mini Kit (Qiagen) and a MagNA Pure LC 2.0 (Roche Diagnostic). An aliquot of the purified DNA was then used for PCR amplification with AmpliTaq Gold[®] polymerase (GE Healthcare Bio-Sciences), biotinylated PGMY09/11 primers to amplify the L1 DNA of mucosal HPVs, and biotinylated HLA primers to amplify cellular HLA DNA. Positive control (0.1 pg/mL of HPV16 DNA as a plasmid) and negative control (dH₂O) were included to verify the sensitivity of PCR and monitor contamination of HPV DNA in reagents. The PCR products were run on 1.5% agarose gels to assign the positivity of HPV DNA amplification and to confirm the integrity of the extracted DNA by amplification of HLA DNA. Reverse blotting hybridization was performed as described (12, 13). Briefly, 15 μ l denatured PCR products were allowed to hybridize with oligonucleotide probes specific for 31 HPV types (HPV6, 11, 16, 18, 26, 31, 33, 34, 35, 39, 40, 42, 44, 45, 51, 52, 53, 54, 55, 56, 57, 58, 59, 66, 68, 69, 70, 73, 82, 83, and 84) immobilized on a Biotin C membrane (Pall corporation) using a Miniblotter MN45 (Immunetics, Cambridge, MA, USA). The hybridized DNA was detected using streptavidin–HRP (GE Healthcare Bio-Sciences, Piscataway, NJ, USA) and the ECL detection reagent (GE Healthcare Bio-Sciences). For adenocarcinoma samples with negative results from the L1 PCR, E6 PCR was performed using PCR Human Papillomavirus Typing Set (Takara, Ohtsu, Japan) that detects HPV16, 18, 31, 33, 35, 52 and 58.

STATISTICAL ANALYSIS

A generalized linear model with binomial distribution and log link was used to calculate the prevalence ratio (PR) of high-risk HPVs between different histological grades with 95% confidence intervals (CI). The PR was adjusted with the

Table 1. Human papillomavirus (HPV) genotype distribution in CIN2/3 in Japanese women

Type	CIN2 (n = 164)	%	CIN3 (n = 334)	%	PR (CIN3 vs. CIN2) (95% CI)	P (Wald test)
High risk						
16	48	29.3	150	44.9	1.62 (1.26–2.13)	0.0003**
18	11	6.7	24	7.2	1.03 (0.53–2.15)	0.93
26	1	0.6	0	0.0	ND	
31	16	9.8	42	12.6	1.30 (0.77–2.32)	0.35
33	6	3.7	15	4.5	1.33 (0.54–3.69)	0.55
35	5	3.0	6	1.8	0.63 (0.19–2.19)	0.45
39	6	3.7	8	2.4	0.67 (0.23–2.03)	0.46
45	4	2.4	3	0.9	0.35 (0.07–1.61)	0.18
51	16	9.8	20	6.0	0.65 (0.34–1.25)	0.18
52	45	27.4	87	26.0	0.93 (0.68–1.28)	0.63
53	10	6.1	4	1.2	0.23 (0.06–0.69)	0.013*
56	9	5.5	8	2.4	0.43 (0.16–1.12)	0.08
58	36	22.0	58	17.4	0.81 (0.56–1.20)	0.28
59	1	0.6	1	0.3	0.41 (0.02–10.5)	0.53
66	3	1.8	3	0.9	0.39 (0.08–1.78)	0.22
68	5	3.0	5	1.5	0.66 (0.18–2.35)	0.51
73	0	0.0	0	0.0	ND	
82	8	4.9	10	3.0	0.66 (0.26–1.72)	0.38
Low risk						
6	3	1.8	6	1.8		
11	2	1.2	0	0.0		
40	1	0.6	0	0.0		
42	1	0.6	0	0.0		
43	0	0.0	0	0.0		
44	1	0.6	0	0.0		
54	2	1.2	2	0.6		
55	4	2.4	2	0.6		
57	0	0.0	0	0.0		
69	3	1.8	1	0.3		
70	2	1.2	1	0.3		
83	0	0.0	1	0.3		
84	0	0.0	2	0.6		
Negative	6	3.7	4	1.2		
Multiple	63	38.4	99	29.6		

Single and multiple infections combined.

** $P < 0.001$; * $P < 0.05$; ND, not determined. Statistically significant values are indicated in boldface.

One case having HPV vaccination history (HPV16, 18, 53 and 58 positive) is included in CIN2.

CIN2, cervical intraepithelial neoplasia Grade 2; CIN3, cervical intraepithelial neoplasia Grade 3; PR, prevalence ratio; CI, confidence interval.

women's age at the time of diagnosis. Pearson's χ^2 test with Yates' continuity correction was used to examine differences in the proportion of HPV infections. Two-sided P values were calculated and considered to be significant at <0.05 . All statistical analyses were performed using R version 2.11.1.

RESULTS

HPV PREVALENCE AND TYPE DISTRIBUTION

Overall, HPV DNA was detected in 158 of the 164 CIN2 cases (96.3%), 330 of the 334 CIN3 cases (98.8%) and 131 of

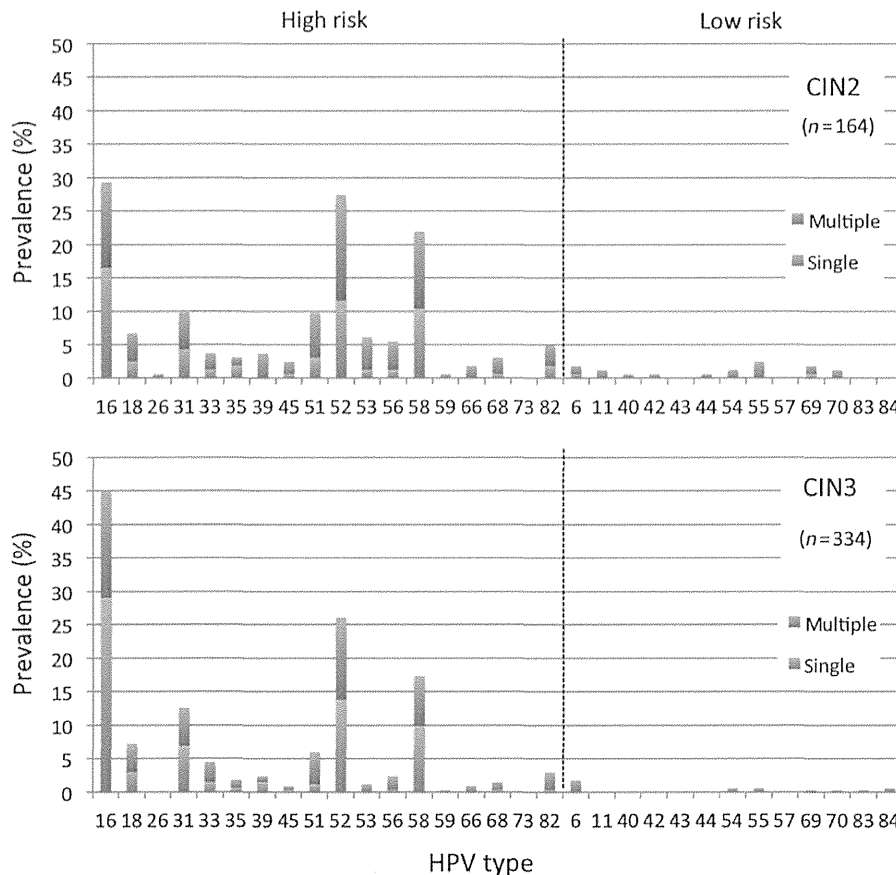


Figure 1. Human papillomavirus (HPV) type distribution in cervical intraepithelial neoplasia (CIN) Grade 2/3 in Japanese women. The proportions of single and multiple infections are presented for individual types. HPV types are grouped as either high- or low-risk based on the risk classification of Munoz et al. (2), except that HPV26 and HPV53 are included in the high-risk group based on phylogenetic classification of the L1 nucleotide sequences.

the 149 ICC cases (87.9%). Table 1 and Figure 1 show the prevalence and genotype distribution of both high- and low-risk HPVs in the CIN2/3 cases that were enrolled in this study. In CIN2 and CIN3, three genotypes, HPV16, HPV52 and HPV58, were predominantly detected among 31 HPV types examined. The proportion of these HPV types in each histological stage was as follows: HPV16 (29.3%), HPV52 (27.4%) and HPV58 (22.0%) in CIN2; HPV16 (44.9%), HPV52 (26.0%) and HPV58 (17.4%) in CIN3. Low-risk HPVs were detected in 18 cases (11.0%) in CIN2 and 14 cases (4.2%) in CIN3, all with other high-risk HPVs except for one case of single-positive HPV6 in CIN2 and one case of single-positive HPV69 in CIN2. The proportion of low-risk HPV infections was significantly lower in CIN3 than in CIN2 ($P = 0.007$, χ^2 test).

In accordance with the distribution patterns observed with CIN2/3 lesions, HPV16 (47.7%) was most frequently detected in ICC, whereas the second common type was HPV18 (23.5%), followed by HPV52 (8.7%) (Table 2). Among the ICC cases, the detection rate of HPV DNA was relatively low in adenocarcinoma (71.4%) compared with squamous cell carcinoma (SCC) (97.8%), and type distributions of high-risk

HPVs were apparently different between the two histological types (Fig. 2), as previously reported (14). Although HPV16 (60.4%) was the most common type in SCC, followed by HPV52 (12.1%) and HPV18 (11.0%), HPV18 (41.1%) was most frequently detected in adenocarcinoma, followed by HPV16 (28.6%) and HPV51 (5.4%).

PREVALENCE RATIO

To evaluate the risk of CIN progression attributable to individual high-risk HPVs, the prevalence ratio (PR) of each high-risk HPV was calculated by comparing the incidence in CIN3 and CIN2. As shown in Table 1, HPV16 prevalence was significantly higher in CIN3 compared with CIN2 (PR = 1.62, 95% CI = 1.26–2.13). Conversely, HPV53 prevalence was negatively associated with progression from CIN2 to CIN3 (PR = 0.23, 95% CI = 0.06–0.69). CIN2/3 and SCC cases positive for HPV16 showed a trend towards younger age compared with HPV16-negative cases (Fig. 3). Indeed, statistical analysis, using a log-binomial model, of high-risk HPVs prevalence in CIN2 and CIN3 with age revealed significantly higher PR with decreasing age for HPV16 (PR/year = 1.03,

Table 2. HPV genotype distribution in ICC in Japanese women

Type	ICC (n = 149)	%	SCC (n = 91)	%	Adc (n = 56)	%	PR (SCC vs. CIN3) (95% CI)	P (Wald test)
High risk								
16	71	47.7	55	60.4	16	28.6	1.55 (1.25–1.87)	0.000007**
18	35	23.5	10	11.0	23	41.1	1.62 (0.72–3.33)	0.20
26	0	0.0	0	0.0	0	0.0	ND	
31	3	2.0	3	3.3	0	0.0	0.23 (0.05–0.65)	0.017*
33	4	2.7	3	3.3	1	1.8	0.70 (0.15–2.22)	0.59
35	2	1.3	2	2.2	0	0.0	1.69 (0.24–7.38)	0.52
39	3	2.0	3	3.3	0	0.0	1.07 (0.20–4.14)	0.93
45	1	0.7	1	1.1	0	0.0	0.98 (0.04–9.24)	0.99
51	3	2.0	0	0.0	3	5.4	ND	
52	13	8.7	11	12.1	2	3.6	0.47 (0.24–0.82)	0.014*
53	1	0.7	0	0.0	0	0.0	ND	
56	3	2.0	2	2.2	1	1.8	0.93 (0.13–3.97)	0.93
58	8	5.4	6	6.6	2	3.6	0.38 (0.15–0.80)	0.024*
59	1	0.7	0	0.0	1	1.8	ND	
66	2	1.3	1	1.1	1	1.8	0.57 (0.02–6.46)	0.69
68	3	2.0	3	3.3	0	0.0	3.26 (0.67–13.0)	0.11
73	0	0.0	0	0.0	0	0.0	ND	
82	0	0.0	0	0.0	0	0.0	ND	
Low risk								
42	1	0.7	0	0.0	1	1.8		
54	3	2.0	3	3.3	0	0.0		
Negative	18	12.1	2	2.2	16	28.6		
Multiple	21	14.1	13	14.3	7	12.5		

Single and multiple infections combined.

** $P < 0.001$; * $P < 0.05$; ND, not determined. Statistically significant values are indicated in boldface.

One adenosquamous carcinoma (HPV18 positive) is included in Adc. One small cell carcinoma (HPV18 positive) and one undifferentiated carcinoma (HPV18/53 positive) included in SCC are excluded from SCC and Adc.

ICC, invasive cervical cancer; SCC, squamous cell carcinoma; Adc, adenocarcinoma; CIN3, cervical intraepithelial neoplasia Grade 3; PR, prevalence ratio; CI, confidence interval.

95% CI = 1.01–1.04, $P = 0.0009$) and for HPV68 (PR/year = 1.13, 95% CI = 1.03–1.27, $P = 0.021$). No significant association with age was observed for prevalence of other high-risk types (data not shown).

When the prevalence of high-risk types was analyzed between CIN3 and SCC, an excess of HPV16 was found in SCC compared with CIN3 (HPV16: PR = 1.55, 95% CI = 1.25–1.87) (Table 2). In contrast, the prevalence of HPV31, HPV52 and HPV58 was significantly decreased in SCC compared with CIN3.

MULTIPLE INFECTIONS

As shown in Figure 4A, multiple infections were detected in 38.4% of the CIN2 cases, 29.6% of the CIN3 cases and 14.1% of the ICC cases, showing a decreasing trend with severity of

lesions, whereas the proportion of single infection increased from 57.9% in CIN2 to 73.8% in ICC. The number of detected HPV types significantly decreases as the lesion develops to ICC ($P = 0.0005$) and with age ($P = 1.3 \times 10^{-6}$). Among multiple infections, the proportion of HPV16 and/or HPV18 infections with other high-risk HPVs was 15.9% in CIN3, which was significantly higher than the 6.7% in ICC ($P = 0.009$), but not significantly different to the 12.2% in CIN2 ($P = 0.34$) (Fig. 4B). The proportion of HPV16 and/or HPV18 infections without other high-risk HPVs was significantly higher in CIN3 than in CIN2 ($P = 0.006$), and was higher still in ICC than in CIN3 ($P = 1.7 \times 10^{-8}$). In contrast, the proportion of high-risk HPV infections other than HPV16/18 was significantly lower in CIN3 than in CIN2 ($P = 0.010$), and was yet lower in ICC than in CIN3 ($P = 1.8 \times 10^{-9}$).

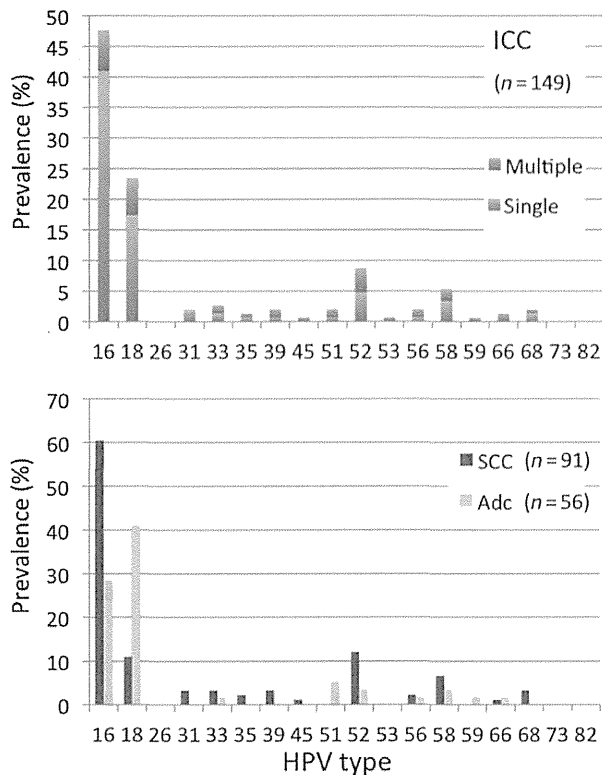


Figure 2. HPV type distribution in invasive cervical cancer (ICC) in Japanese women. The prevalence of single and multiple infections in ICC for individual types (upper panel). The type distribution in squamous cell carcinoma (SCC) and adenocarcinoma (Adc) (lower panel).

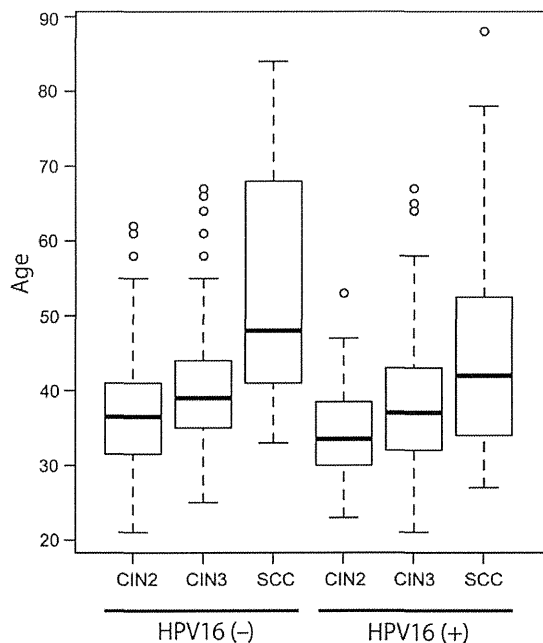


Figure 3. Association of age with HPV16 positivity in CIN2/3 and SCC.

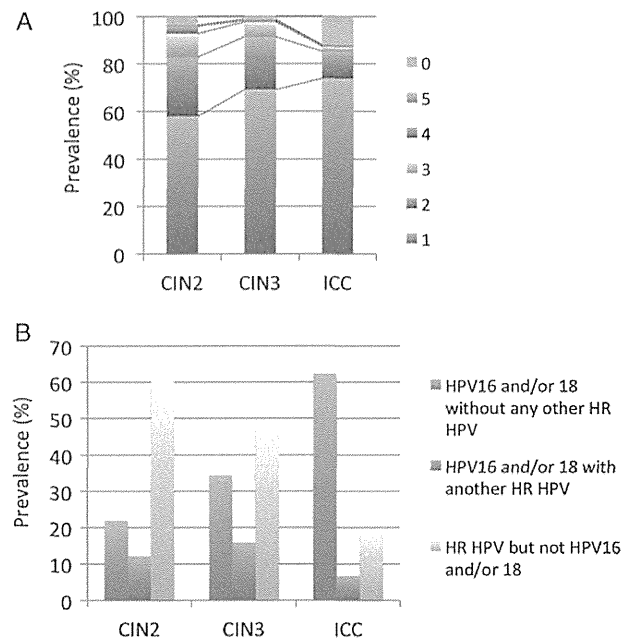


Figure 4. Multiple HPV infections in CIN2/3 and ICC in Japanese women. (A) The distribution of the number of HPV types detected for each histological grade. (B) The prevalence of HPV16 and/or 18 and other high-risk HPV, alone or in mixed infections with HPV16 and/or 18, for each histological grade.

With regard to the three most frequent types detected in CIN2/3, the proportion of co-infections was as follows: in CIN2, HPV16/52 in 8 cases (4.9%), HPV16/58 in 4 cases (2.4%), and HPV52/58 in 8 cases (4.9%); in CIN3, HPV16/52 in 14 cases (4.2%), HPV16/58 in 9 cases (2.7%), and HPV52/58 in 8 cases (2.4%) (Fig. 5). Triple-infections were found in two cases of CIN2 and in one case of CIN3.

DISCUSSION

Here we have presented the prevalence and type distribution of high-risk HPVs in cervical precancerous lesions and ICC in Japan using a validated genotyping method. A number of studies have so far been conducted to investigate the HPV type distribution in Japanese women (8–10, 15–19), but most of those studies depended on HPV typing performed at each hospital laboratory and only a limited number utilized a centralized external laboratory with quality assurance of its testing capability. Since our typing capability using the PGMY-line blot assay has been consistently evaluated as proficient in the HPV DNA proficiency panel studies conducted annually by the WHO HPV laboratory network (20), the results obtained in this study provide the most recent and reliable pre-vaccination baseline data for Japanese HPV infection.

In a meta-analysis assembling HPV genotyping data from 984 ICC cases in Japan, the top three HPV types were HPV16 (44.8%), HPV18 (14.0%), and HPV52 (7.0%) (7). The

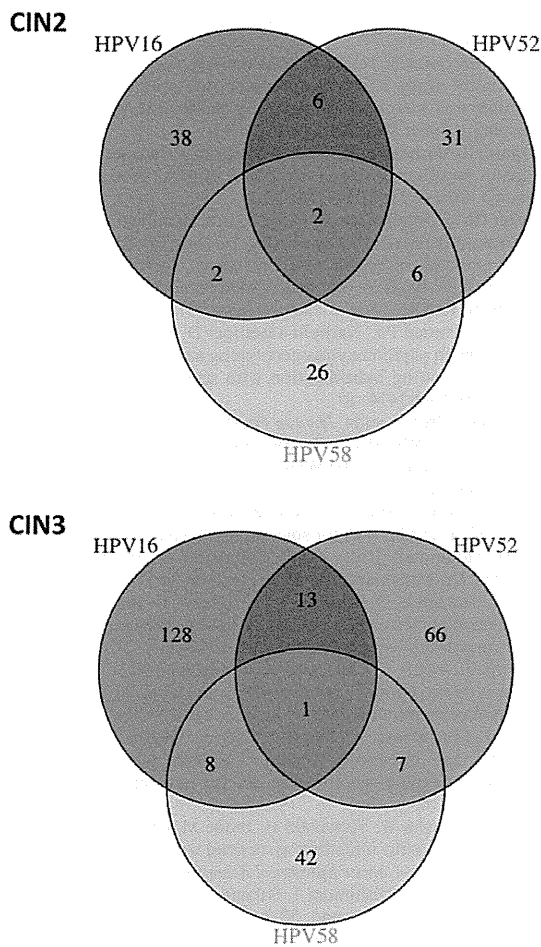


Figure 5. Venn diagram showing the overlap of HPV16/52/58 infections in CIN2 (A) and CIN3 (B). The number in circles indicates the number of subjects positive for HPV16 and/or HPV52 and/or HPV58.

observed distribution of high-risk HPVs in ICC reported in this study is almost similar, suggesting that the general trend for causative HPV types in ICC has not dramatically changed in Japan. The type distributions in SCC and adenocarcinoma found in this study are also similar to those reported in the previous meta-analysis (7), in which the top three most frequent HPV types were HPV16 (45.8%), HPV18 (10.8%) and HPV52 (7.4%) in SCC, and HPV18 (58.2%), HPV16 (31.3%) and HPV68 (4.5%) in adenocarcinoma. However, HPV68 was not detected in adenocarcinoma in this study.

Compared with the high HPV positivity in SCC (97.8%), the low HPV detection rate observed in adenocarcinoma (71.4%) is consistent with a recent study summarizing HPV genotyping data for cervical adenocarcinoma (21), which demonstrated that the positivity rate of HPV DNA in adenocarcinoma ranged from 65.6% (6) to 82.0% (22). The HPV-negative adenocarcinoma cases ($n = 16$) in this study were further examined by PCR targeting the HPV E6 gene, but again no HPV DNA was amplified from these samples

(data not shown). The low detection rate of HPV DNA may be due to HPV integration into the host genome that disrupts the L1 and E6 genes used for HPV typing, improper sampling of endocervical cells, or degradation of cell samples containing low levels of HPV DNA. The low HPV positivity in cervical adenocarcinoma may also be attributed to the presence of inherently HPV-unrelated glandular lesions. In support of this notion, gastric-type adenocarcinoma, which exhibits a range of phenotypic gastric differentiation, has recently been proposed as another subtype of cervical adenocarcinoma and shown to be unrelated to HPV infection (23). Nevertheless, gastric-type adenocarcinoma was not found in the adenocarcinoma cases in this study.

The HPV type distribution in CIN2/3 in this study shows similar patterns to that previously reported by Onuki et al. (17), in which the top three most frequent types were HPV16 (24.1%), HPV52 (17.5%) and HPV58 (10.7%). Thus, the results in this study strongly support a major role for HPV16, HPV52 and HPV58 in causing CIN2/3 in Japanese women.

A recent prospective study followed Japanese women with low-grade cervical lesions and estimated the risk of disease progression associated with high-risk HPV infections (24). That study reported hazard ratios of individual high-risk types for progression to CIN3; 7 HPV types (HPV16, 18, 31, 33, 35, 52 and 58) showed a high risk of progression. Consistent with these findings, in our study HPV16 exhibited significantly higher PR in CIN3 compared with CIN2, suggesting a higher potential for progression from CIN2 to CIN3 than with other high-risk types. Faster progression of HPV16-infected lesions to CIN3 can also explain the observed association of younger age with the development of HPV16-positive CIN3. The high PR of HPV16 in SCC compared with CIN3 lends further support to the increased carcinogenicity of persistent HPV16 infection. In contrast, we found a low prevalence of HPV31, HPV52 and HPV58 in SCC compared with CIN3, which suggests a lower potential for progression to SCC than with HPV16 infection.

Multiple infections were more frequently detected in CIN2/3 in our results than in those reported by Onuki et al. (11.3% in CIN2/3) (17). This difference likely reflects the higher sensitivity of the PGMV-lineblot genotyping methodology to detect multiple infections, without inter-type PCR competition, as previously reported (25). Alternatively, the high prevalence of multiple infections might result from using cervical exfoliated cell instead of tissue sections containing CIN2/3 lesions. However, multiple infections with high-risk types have previously been reported in a study using tissue sections from cervical biopsies (26).

Caution should be taken regarding co-infections of HPV16/18 with other high-risk types, because currently available vaccines targeting HPV16/18 exhibit only limited cross protection against infections with other high-risk HPVs (3). We report a substantial proportion of HPV16/18 co-infections with other high-risk HPVs in CIN3 (Fig. 4B), a proportion that is significantly higher than that in ICC. Although a causative HPV type for CIN3 lesions is difficult to determine when

co-infections are detected, the co-infection may still progress to ICC via the other high-risk types if HPV16/18 infections were prevented by vaccination. Of particular concern is the fact that HPV52 and HPV58 are commonly detected in East Asian countries and we report a significant number of co-infections between HPV52/58 and HPV16 in CIN2/3 in Japanese women (Fig. 5). Therefore, there is a possibility of an increase in the incidence of HPV52/58-positive ICC if HPV16/18 infections are prevented. Thus, careful monitoring of these genotypes in CIN2/3 lesions will be required after the widespread introduction of HPV vaccines into Japan and other East Asian countries in order to evaluate the overall efficacy of HPV vaccination.

Acknowledgement

We thank Dr Tadahito Kanda for critical reading of the manuscript.

Funding

This study was supported by funding from the Ministry of Health, Labor, and Welfare in Japan.

Conflict of interest statement

None declared.

References

1. The FUTUREII Study Group. Quadrivalent vaccine against human papillomavirus to prevent high-grade cervical lesions. *N Engl J Med* 2007;356:1915–27.
2. Munoz N, Bosch FX, de Sanjose S, Herrero R, Castellsague X, et al. Epidemiologic classification of human papillomavirus types associated with cervical cancer. *N Engl J Med* 2003;348:518–27.
3. Schiller JT, Castellsague X, Garland SM. A review of clinical trials of human papillomavirus prophylactic vaccines. *Vaccine* 2012; 30(Suppl 5):F123–138.
4. Parkin DM, Louie KS, Clifford G. Burden and trends of type-specific human papillomavirus infections and related diseases in the Asia Pacific region. *Vaccine* 2008; 26(Suppl 12):M1–16.
5. Konno R, Shin HR, Kim YT, Song YS, Sasagawa T, et al. Human papillomavirus infection and cervical cancer prevention in Japan and Korea. *Vaccine* 2008; 26(Suppl 12):M30–42.
6. de Sanjose S, Quint WG, Alemany L, Geraets DT, Klaustermeier JE, et al. Human papillomavirus genotype attribution in invasive cervical cancer: a retrospective cross-sectional worldwide study. *Lancet Oncol* 2010;11:1048–56.
7. Miura S, Matsumoto K, Oki A, Satoh T, Tsunoda H, et al. Do we need a different strategy for HPV screening and vaccination in East Asia? *Int J Cancer* 2006;119:2713–5.
8. Yoshikawa H, Kawana T, Kitagawa K, Mizuno M, Yoshikura H, et al. Detection and typing of multiple genital human papillomaviruses by DNA amplification with consensus primers. *Jpn J Cancer Res* 1991;82:524–31.
9. Asato T, Maehama T, Nagai Y, Kanazawa K, Uezato H, et al. A large case–control study of cervical cancer risk associated with human papillomavirus infection in Japan, by nucleotide sequencing-based genotyping. *J Infect Dis* 2004;189:1829–32.
10. Nakagawa S, Yoshikawa H, Onda T, Kawana T, Iwamoto A, et al. Type of human papillomavirus is related to clinical features of cervical carcinoma. *Cancer* 1996;78:1935–41.
11. Wheeler CM, Castellsague X, Garland SM, Szarewski A, Paavonen J, et al. Cross-protective efficacy of HPV-16/18 AS04-adjuvanted vaccine against cervical infection and precancer caused by non-vaccine oncogenic HPV types: 4-year end-of-study analysis of the randomised, double-blind PATRICIA trial. *Lancet Oncol* 2012;13:100–10.
12. Estrade C, Menoud PA, Nardelli-Haeffliger D, Sahli R. Validation of a low-cost human papillomavirus genotyping assay based on PGMV PCR and reverse blotting hybridization with reusable membranes. *J Clin Microbiol* 2011;49:3474–81.
13. World Health Organization. *Human Papillomavirus Laboratory Manual*. 1st edn. (WNO/IVB/10.12) Geneva, Switzerland: WHO 2009. http://whqlibdoc.who.int/hq/2010/WHO_IVB_10.12_eng.pdf (15 August 2014, date last accessed).
14. Bulk S, Berkhof J, Bulkman NW, Zielinski GD, Rozendaal L, et al. Preferential risk of HPV16 for squamous cell carcinoma and of HPV18 for adenocarcinoma of the cervix compared to women with normal cytology in The Netherlands. *Br J Cancer* 2006;94:171–5.
15. Konno R, Tamura S, Dobbelaere K, Yoshikawa H. Prevalence and type distribution of human papillomavirus in healthy Japanese women aged 20 to 25 years old enrolled in a clinical study. *Cancer Sci* 2011;102:877–82.
16. Maehama T, Asato T, Kanazawa K. Prevalence of HPV infection in cervical cytology-normal women in Okinawa, Japan, as determined by a polymerase chain reaction. *Int J Gynaecol Obstet* 2000;69:175–6.
17. Onuki M, Matsumoto K, Satoh T, Oki A, Okada S, et al. Human papillomavirus infections among Japanese women: age-related prevalence and type-specific risk for cervical cancer. *Cancer Sci* 2009;100:1312–6.
18. Sasagawa T, Basha W, Yamazaki H, Inoue M. High-risk and multiple human papillomavirus infections associated with cervical abnormalities in Japanese women. *Cancer Epidemiol Biomarkers Prev* 2001;10:45–52.
19. Takehara K, Toda T, Nishimura T, Sakane J, Kawakami Y, et al. Human papillomavirus types 52 and 58 are prevalent in uterine cervical squamous lesions from Japanese women. *Pathol Res Int* 2011;2011:246936.
20. Eklund C, Zhou T, Dillner J. Global proficiency study of human papillomavirus genotyping. *J Clin Microbiol* 2010;48:4147–55.
21. Pimenta JM, Galindo C, Jenkins D, Taylor SM. Estimate of the global burden of cervical adenocarcinoma and potential impact of prophylactic human papillomavirus vaccination. *BMC Cancer* 2013;13:553.
22. Li N, Franceschi S, Howell-Jones R, Snijders PJ, Clifford GM. Human papillomavirus type distribution in 30,848 invasive cervical cancers worldwide: Variation by geographical region, histological type and year of publication. *Int J Cancer* 2011;128:927–35.
23. Mikami Y, McCluggage WG. Endocervical glandular lesions exhibiting gastric differentiation: an emerging spectrum of benign, premalignant, and malignant lesions. *Adv Anat Pathol* 2013;20:227–37.
24. Matsumoto K, Oki A, Furuta R, Maeda H, Yasugi T, et al. Predicting the progression of cervical precursor lesions by human papillomavirus genotyping: a prospective cohort study. *Int J Cancer* 2011;128:2898–910.
25. Mori S, Nakao S, Kukimoto I, Kusumoto-Matsuo R, Kondo K, et al. Biased amplification of human papillomavirus DNA in specimens containing multiple human papillomavirus types by PCR with consensus primers. *Cancer Sci* 2011;102:1223–7.
26. Howell-Jones R, Bailey A, Beddows S, Sargent A, de Silva N, et al. Multi-site study of HPV type-specific prevalence in women with cervical cancer, intraepithelial neoplasia and normal cytology, in England. *Br J Cancer* 2010;103:209–16.

Matrix Metalloproteinase (MMP)-9 in Cancer-Associated Fibroblasts (CAFs) Is Suppressed by Omega-3 Polyunsaturated Fatty Acids *In Vitro* and *In Vivo*

Ayumi Taguchi¹, Kei Kawana^{1*}, Kensuke Tomio¹, Aki Yamashita¹, Yosuke Isobe², Kazunori Nagasaka¹, Kaori Koga¹, Tomoko Inoue¹, Haruka Nishida¹, Satoko Kojima¹, Katsuyuki Adachi¹, Yoko Matsumoto¹, Takahide Arimoto¹, Osamu Wada-Hiraike¹, Katsutoshi Oda¹, Jing X. Kang³, Hiroyuki Arai², Makoto Arita^{2*}, Yutaka Osuga¹, Tomoyuki Fujii¹

1 Department of Obstetrics and Gynecology, Graduate School of Medicine, The University of Tokyo, 7-3-1 Hongo, Bunkyo-ku, Tokyo, Japan, **2** Department of Health Chemistry, Graduate School of Pharmaceutical Sciences, The University of Tokyo, 7-3-1 Hongo, Bunkyo-ku, Tokyo, Japan, **3** Department of Medicine, Massachusetts General Hospital and Harvard Medical School, Charlestown, Massachusetts, United States of America

Abstract

Cancer associated fibroblasts (CAFs) are responsible for tumor growth, angiogenesis, invasion, and metastasis. Matrix metalloproteinase (MMP)-9 secreted from cancer stroma populated by CAFs is a prerequisite for cancer angiogenesis and metastasis. Omega-3 polyunsaturated fatty acids (omega-3 PUFA) have been reported to have anti-tumor effects on diverse types of malignancies. Fat-1 mice, which can convert omega-6 to omega-3 PUFA independent of diet, are useful to investigate the functions of endogenous omega-3 PUFA. To examine the effect of omega-3 PUFA on tumorigenesis, TC-1 cells, a murine epithelial cell line immortalized by human papillomavirus (HPV) oncogenes, were injected subcutaneously into fat-1 or wild type mice. Tumor growth and angiogenesis of the TC-1 tumor were significantly suppressed in fat-1 compared to wild type mice. cDNA microarray of the tumors derived from fat-1 and wild type mice revealed that MMP-9 is downregulated in fat-1 mice. Immunohistochemical study demonstrated immunoreactivity for MMP-9 in the tumor stromal fibroblasts was diffusely positive in wild type whereas focal in fat-1 mice. MMP-9 was expressed in primary cultured fibroblasts isolated from fat-1 and wild type mice but was not expressed in TC-1 cells. Co-culture of fibroblasts with TC-1 cells enhanced the expression and the proteinase activity of MMP-9, although the protease activity of MMP-9 in fat-1-derived fibroblasts was lower than that in wild type fibroblasts. Our data suggests that omega-3 PUFAs suppress MMP-9 induction and tumor angiogenesis. These findings may provide insight into mechanisms by which omega-3 PUFAs exert anti-tumor effects by modulating tumor microenvironment.

Citation: Taguchi A, Kawana K, Tomio K, Yamashita A, Isobe Y, et al. (2014) Matrix Metalloproteinase (MMP)-9 in Cancer-Associated Fibroblasts (CAFs) Is Suppressed by Omega-3 Polyunsaturated Fatty Acids *In Vitro* and *In Vivo*. PLoS ONE 9(2): e89605. doi:10.1371/journal.pone.0089605

Editor: Zhongjun Zhou, The University of Hong Kong, Hong Kong

Received: October 10, 2013; **Accepted:** January 22, 2014; **Published:** February 27, 2014

Copyright: © 2014 Taguchi et al. This is an open-access article distributed under the terms of the Creative Commons Attribution License, which permits unrestricted use, distribution, and reproduction in any medium, provided the original author and source are credited.

Funding: This study was funded by Tokyo IGAKUKAI (K.K.), the Japan Science and Technology Agency Precursory Research for Embryonic Science and Technology (PRESTO) (M.A.), the Ministry of Education, Culture, Sports, Science, and Technology of Japan (M.A.). The funders had no role in study design, data collection and analysis, decision to publish, or preparation of the manuscript.

Competing Interests: The authors have declared that no competing interests exist.

* E-mail: kkawana-ky@umin.org (K. Kawana); marita@mol.f.u-tokyo.ac.jp (MA)

These authors contributed equally to this work.

Introduction

The tumor microenvironment is comprised of microvascular endothelial cells, adjacent normal epithelial cells and cancer-associated fibroblasts (CAFs), and is reported to be an important regulator of tumorigenesis [1,2]. As the most common cellular population found in the tumor microenvironment, CAFs are responsible for the synthesis of proteins involved in the remodeling of the extracellular matrix (ECM), and for the secretion of growth factors and cytokines that regulate tumor cell proliferation and invasion [3,4]. In murine ovarian cancer xenograft models, the p53/NF-κB pathway in CAFs significantly increased *in vivo* tumor growth [5]. In colon cancer, Zhu Y et al. report that IL-1β increased colon cancer cell proliferation and invasion by up-regulating COX-2 signaling in CAFs [6].

Matrix-metalloproteinases (MMPs) are synthesized as proenzymes and typically activated by proteolytic removal of a propeptide [7]. MMPs are reported to influence tumor progression by facilitating events pivotal for neovascularization and establishment of distant metastasis including proliferation, survival and migration of endothelial, tumor and stromal cells [8,9]. MMP-2 and MMP-9 are implicated as prerequisites for angiogenesis and metastasis in the carcinogenic process. MMP-2 is expressed in the various cancer cell lines [10]. In contrast, MMP-9 has very limited or no expression in these cancer cells. Instead, MMP-9 is well-known to be secreted from cancer stromal fibroblasts and endothelial cells [11,12]. MMP-9 is a member of a family of zinc containing endoproteases that is involved in degradation of extracellular matrix (ECM) and in vascular remodeling [13].

Docosahexaenoic acid (DHA, 22:6n-3) and eicosapentaenoic acid (EPA, 20:5n-3) are representative mediators of omega-3

polyunsaturated fatty acids (omega-3 PUFAs) and exert anti-inflammatory effects in acute and chronic pathological inflammatory reactions by counteracting inflammation [14]. Omega-3 PUFAs are also reported to have anti-cancer effects based on in vitro and vivo studies [15–17]. Several mechanisms have been proposed to explain the anti-cancer effects of omega-3 PUFAs. Omega-3 PUFAs alter the growth of tumor cells by modulating cell replication, by interfering with components of the cell cycle or by increasing cell death via necrosis or apoptosis [18,19]. Omega-3 PUFAs are also known to exert anti-angiogenic effects by inhibiting the production of many angiogenic mediators including: vascular endothelial growth factor (VEGF), platelet-derived growth factor (PDGF), and prostaglandin E2 (PGE2) [20–24].

Dietary supplementation is a traditional approach to modify tissue nutrient composition in animal studies of nutrition. Feeding animals diets that alter specific nutritional and non-nutritional components can help to differentiate experimental groups; however, it can be exceedingly difficult to provide diets that are identical in all but a single or a small but controlled number of components. Kang et al. recently engineered a transgenic mouse that carries the fat-1 gene from the roundworm *Caenorhabditis elegans* [25]. This gene encodes an omega-3 fatty acid desaturase that catalyzes the conversion of omega-6 to omega-3 PUFAs and that is absent in most animals, including mammals. There is a remarkable difference in the tissue omega-6/omega-3 PUFA ratio between wild type and fat-1 transgenic mice [26]. Fat-1 mice, which typically exhibit a balanced ratio of omega-6 to omega-3 PUFAs in their tissues and organs independent of diet, allow carefully controlled studies to be performed in the absence of potential confounding factors of diet. This makes them a useful model to investigate the biological properties of endogenous omega-3 PUFAs [25]. Several reports using fat-1 mice have demonstrated anti-cancer effects of omega-3 PUFAs [27–30]. In these investigations, omega-3 PUFAs exerted anti-cancer effects by suppressing inflammatory reactions and PGE2 secretion from cancer cells. To date, there are few studies that investigate the involvement of omega-3 PUFAs in the biology of CAFs.

In this study, we hypothesized that omega-3 PUFAs may alter tumor microenvironments by influencing CAF activity. To examine this hypothesis, fibroblasts derived from fat-1 and wild type mice were assessed both in vitro and in vivo under conditions allowing interaction with TC-1 cancer cells. TC-1 cells were derived from the epithelium of C56BL/6 mice and immortalized by human papillomavirus (HPV) type 16 E6 and E7 oncoproteins. They are commonly used in vitro and in vivo in murine models of HPV-related cancer [31]. Here, we investigated the involvement of omega-3 PUFAs in TC-1 tumorigenesis by comparing fat-1 and wild type mice. Our specific focus involved the study of tumor-associated fibroblasts. These models are useful in the study of CAFs because the cancer cells originate in wild type murine epithelium while the cancer stromal components, including CAFs, come from fat-1 (omega-3 PUFAs-rich) or wild type (normal PUFAs) mice.

Materials and Methods

Animals and diet

Fat-1 mice were created on a C57BL/6 background as described [26] and subsequently backcrossed (at least four times) onto a C57BL/6 background. Animals were fed a special diet (AIN-76A+10% safflower oil; CLEA Japan, Inc.) that contained 10.3% total fat with fatty acid composition of C16:0 (7.6%), C18:0 (2.7%), C18:1n-9 (14.1%), C18:2n-6 (73.2%), C18:3n-3 (0.3%), C20:4n-6 (<0.1%), C20:5n-3 (<0.1%), C22:6n-3 (<0.1%), high

in n-6 and low in n-3 fatty acids, until the desired age (6–8 weeks) for experiments. To prevent the oxidation of lipids in the diet, all foods were stored in the refrigerator with antioxidants (AGELESS; Mitsubishi Gas Chemical Inc.), and prepared newly every two days. Animal studies were approved by the University of Tokyo Animal Committee.

Tumor growth assay in mice

TC-1 cells are derived from a primary lung epithelial cell from C56BL6/mice and immortalized using HPV 16 E6/E7 plus c-Has-ras (kind gift from Dr. T. C. Wu, Johns-Hopkins University, Baltimore MD USA) [32]. TC-1 cells were cultured in DMEM (Gibco, NY, USA) containing 10% FBS, 100 U/ml penicillin, 0.1 mg/ml streptomycin, and 0.25 g/ml amphotericin B. Eight-week-old female mice were injected with 5×10^6 murine TC-1 cells suspended in 100 μ l of DMEM. Tumor volume, based on caliper measurements, was calculated at 7 and 14 days after injection according to the following formula: (tumor volume) = $1/2 \times (\text{the shortest diameter})^2 \times (\text{the largest diameter})$. Mice were sacrificed 14 days after inoculation, tumors were excised and stored at -80°C for future analyses.

cDNA microarray

Total RNA from TC-1 tumors (above) was extracted using an RNeasy minikit (QIAGEN, Hilden, Germany). For the cDNA microarray analysis, 0.5 μ g of pooled total RNA was amplified and labeled using an Amino Allyl MessageAmp™ II mRNA Amplification kit (Applied Biosystems, Foster City, CA, USA) according to the manufacturer's instructions. Each sample of mRNA labeled with Cy3 and reference mRNA labeled with Cy5 was cohybridized to the Gene™ Mouse Oligo chip 24 k (Toray Industries Inc., Tokyo, Japan) at 37°C for 16 h. After hybridization, each DNA chip was washed and dried. Hybridization signals derived from Cy3 and Cy5 were scanned using Scan Array Express (PerkinElmer, Waltham, MA, USA). The scanned image was analyzed using GenePix Pro (MDS Analytical Technologies, Sunnyvale, CA, USA). All analyzed data were scaled by global normalization. GEO accession number is GSE54079.

Immunohistochemistry

Paraffin sections (4 μ m) of TC-1 tumors were dewaxed in xylene and rehydrated through graded ethanol to water. Antigens were retrieved by boiling in 10 mM citrate buffer (pH 6.0) for 30 min. The cooled sections were incubated in DAKO REAL Peroxidase-Blocking solution (DAKO, Carpinteria, CA, USA) for 10 min to quench endogenous peroxidase. To block nonspecific binding, sections were incubated in DAKO Protein Blocking solution (DAKO) for 10 min at room temperature. Sections were then incubated with a rabbit polyclonal antibody against mouse MMP-9 (PAB12714, Abnova, 1:100 dilution) in DAKO REAL Antibody Diluent (DAKO) overnight at 4°C . The slides were incubated for 1 hour at room temperature with peroxidase-conjugated secondary antibodies, washed, incubated with DAB, counterstained with hematoxylin, dehydrated through an ethanol series and xylene, and mounted. To evaluate tumor microvessel formation, tumor sections were stained for CD-31 using a rat monoclonal antibody against mouse CD-31 (ab56299, Abcam, Tokyo, Japan, 1:100 dilution).

RT-quantitative PCR (RT-qPCR)

Total RNA was extracted from TC-1 tumors and cultured fibroblasts using an RNeasy minikit (QIAGEN, Hilden, Germany), followed by reverse transcription. cDNA was amplified for

40 cycles in a Light Cycler 480 (Roche, Basel, Switzerland) using a Universal Probe Master Mix and the following primers and Universal Probe Library (UPL) probes (Roche). The primer pairs and the universal probes corresponding to the each primer that were used in amplifications were as follows: mouse β -actin, 5'-ATTGAAACATCAGCCAAGACC-3' and 5'-CCGAATCTCA-CGGACTAGTGT-3' probe88; mouse MMP-9, 5'-ACGACA-TAGACGGCATCCA-3' and 5'-GCTGTGGTTCAGTTGTG-GTG-3' probe19. Expression of MMP-9 was normalized using β -actin mRNA as an internal standard. Expression levels were calculated by the comparative Ct method using β -actin as an endogenous reference gene.

Primary fibroblast culture and co-culture with TC-1 cells

Lungs were isolated from fat-1 transgenic and wild type mice and washed with saline to remove blood cells. Isolation and culture of pulmonary fibroblasts were performed using methods described previously [33]. Lung tissues were minced into small pieces and incubated in DMEM (Gibco, NY, USA) containing type I collagenase (0.25%; Sigma-Aldrich, St Louis, MO, USA) and deoxynuclease I (15 U/ml; TaKaRa, Tokyo, Japan) for 120 min at 37°C. The resultant dispersed cells were separated by filtration through nylon cell strainers (70 μ m, BD, Franklin Lakes, NJ, USA). Fibroblasts in the filtrate were collected, placed into 10 cm dishes in DMEM containing 10% FBS, 100 U/ml penicillin, 0.1 mg/ml streptomycin, and 0.25 mg/ml amphotericin B, and incubated for 7–10 days. Fibroblasts were purified from other cell population by differential adhesion and serial passage.

Confluent fibroblasts and TC-1 cells were trypsinized and resuspended in DMEM containing 10% FBS, 100 U/ml penicillin, 0.1 mg/ml streptomycin, and 0.25 g/ml amphotericin B and 1×10^5 cells/ml cells of each cell type were plated together in 12 well culture plates. Co-cultures were incubated at 37°C 5% CO₂ in a humidified atmosphere for 24 hours. Homotypic cultures served as controls.

Gelatin zymography

Gelatin zymography assays were performed using a Gelatin zymography kit (Cosmobio, Sapporo, Japan) according to the manufacture's instructions. Cell culture supernatants were collected and centrifuged at 1,500 rpm for 5 minutes. The cell free supernatant was mixed with 2 \times sample buffer and electrophoresed using precast gels (10% polyacrylamide, 0.1% gelatin) at 4°C for 1 hour. Subsequent enzymatic reactions were performed at 37°C overnight. Gelatinase activities were visualized using specific staining solutions and destained in acetic acid-methanol-dH₂O (1:3:6). For semi-quantitative analyses, gelatin zymography bands were analyzed using image analysis software (ImageJ).

Statistical analysis

Data are presented as means \pm SEM. Statistical analyses were carried out by Student's *t*-test, or Wilcoxon analysis using JMP software. A value of $P < 0.05$ was considered significant. In the figure legends, asterisks indicate those comparisons with statistical significance ($p < 0.05$).

Results

Tumor growth and angiogenesis of TC-1 tumors is suppressed in fat-1 mice

To investigate the effect of omega-3 PUFAs on cervical cancer tumorigenesis, we injected TC-1 cells subcutaneously into fat-1 and the litter-mate wild type C57/BL6 mice. TC-1 tumor formation rates and tumor growth were assessed by the number

of mice forming tumors and three-dimension tumor sizes, respectively. There was no difference in tumor formation rates between fat-1 and wild type mice. TC-1 tumor sizes were plotted for 14 days in fat-1 and wild-type controls (Fig. 1). Tumor growth rates were consistently lower in fat-1 mice when compared to wild type mice at all time points. In fat-1 mice, tumor size at 14 days after injection was significantly smaller than in wild-type controls (Fig. 1). Although cell growth of TC-1 cells is dependent on HPV16 E6/E7 expression, E6 and E7 expression in TC-1 tumors was not downregulated in fat-1 mice (Fig. S1).

To further delineate mechanisms behind these differences in tumor growth in this model, particularly in terms of the possible role of host-derived cancer-associated stromal components including CAFs, we next examined whether omega-3 PUFAs modified angiogenesis in TC-1 tumor. We assessed semi-quantitatively tumor microvessel density in TC-1 tumors derived from fat-1 and wild type mice by counting the number of CD31-positive microvessels in immunohistochemical assay (Fig. 2A and 2B). CD31 immunostaining of TC-1 tumors derived from fat-1 and wild type mice (Fig. 2A) demonstrated hypovascularity of the fat-1-derived TC-1 tumors when compared with wild type-derived tumors. The number of CD31-positive microvessels per high-power field in fat-1 mice was significantly lower than that in wild type mice (Fig. 2B). These *in vivo* data indicated that TC-1 tumor growth and angiogenesis were at least suppressed in fat-1 mice when compared with wild type counterparts although it was difficult to accurately estimate TC-1 cell growth in fat-1 mice.

MMP-9 is downregulated in fat-1 mice-derived TC-1 tumors

To investigate potential differences in gene expression profiles of TC-1 tumors growing in the skin of fat-1 and wild type mice, TC-1 tumor tissues obtained from fat-1 and wild type mice were analyzed by cDNA microarray. Since omega-3 PUFAs are reported to influence cell proliferation and inflammation, Table 1 lists relative gene expression levels for representative genes associated with the tumor growth and inflammation (Table 1). With the exception of EGF, expression levels of almost all inflammatory cytokines/chemokines and growth factors in TC-1

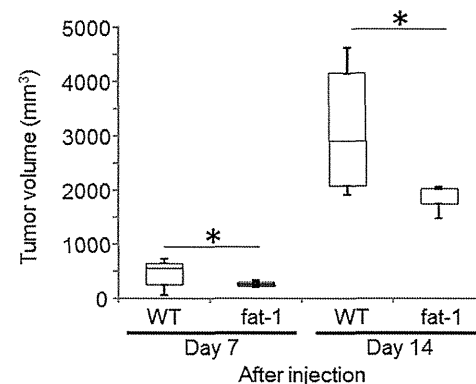


Figure 1. Tumor growth rates in fat-1 and wild type (WT) mice. 5×10^6 murine TC-1 cells suspended in 100 μ l of DMEM were injected s.c. into each of 10 fat-1 and wild type mice. Tumor volume, based on caliper measurements, was calculated at 7 and 14 days after injection according to the following formula: (tumor volume) = $1/2 \times (\text{the shortest diameter})^2 \times (\text{the largest diameter})$. Mean values with standard deviations are presented. Asterisks indicate those comparisons (fat-1 vs. wild type mice) with statistical significance ($p < 0.05$). doi:10.1371/journal.pone.0089605.g001

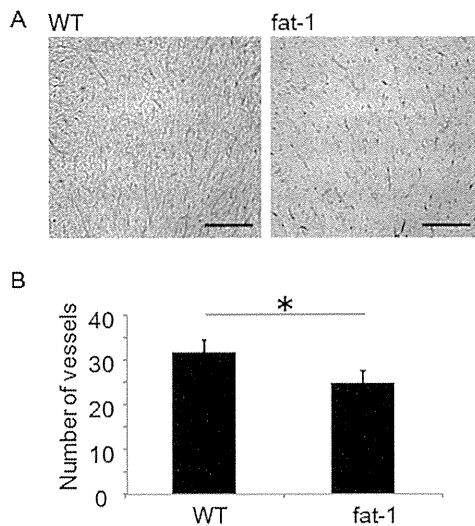


Figure 2. Omega-3 PUFAs suppress tumor vasculogenesis. CD31 immunostaining of the TC-1 tumor derived from wild type (WT) mice (A) and fat-1 (B). Bars indicate 200 μ m. (C) Microvessel densities in TC-1 tumors are expressed as the representative number of labeled vessels in 4 fields (n=5). Mean values with standard deviations are presented. Asterisks indicate those comparisons (fat-1 vs. wild type mice) with statistical significance ($p<0.05$). doi:10.1371/journal.pone.0089605.g002

tumors from fat-1 mice were higher than those, in tumors from wild-type controls. This suggested that anti-inflammatory and anti-cell growth effects of omega-3 PUFAs are unlikely to be central to their anti-tumor activities, at least in this model. We next examined the expression of MMPs in these TC-1 tumors to further address stroma-related angiogenesis in the tumor micro-environments (Table 1). cDNA microarray demonstrated that the expression of MMP-2 and -9 were suppressed in fat-1 mice-derived TC-1 tumor while those of other MMPs were tended to be upregulated when compared to controls. To confirm these effects at the RNA level, RT-qPCR for MMP-9 was performed. MMP-9 RNA levels in fat-1 mice were approximately 60% lower than those in wild type controls (Fig. 3A). TC-1 tumor immunohistochemistry confirmed these results at the protein level. MMP-9 immunoreactivity in wild type mouse-derived TC-1 tumors was clearly stronger than fat-1 mouse-derived tumors (Fig. 3B). High power histochemical analysis of MMP-9 immunoreactivity in TC-1 cells (Fig. 3B, inserts) revealed negligible expression, while that of the stromal components including CAFs and endothelial cells was strongly positive only in the wild type-derived TC-1 tumors. These data indicated that the production of MMP-9 in CAFs and endothelial cells was clearly suppressed in fat-1 mice.

MMP-9 expression and gelatinase activity were suppressed in cultured primary fibroblasts derived from fat-1 mice

To mimic the cancer stromal microenvironment in vitro, we co-cultured fibroblasts isolated from fat-1 and wild type mice with TC-1 cells. We used lung tissues from fat-1 and wild type mice as the sources for fibroblasts, and differential adhesion methodology for their isolation. All fibroblasts were passaged 3–4 times prior to use in experiments. Baseline MMP-9 expression levels in primary fibroblasts from fat-1 mice were approximately 60% lower than those from wild type-derived fibroblasts (Fig. 4A). Culture

Table 1. Cytokine, growth factor, and MMP gene expression comparisons in TC-1 tumors from fat-1 vs wild type mice.

Genes	fat-1/WT ratio
EGF	0.4
CXCL-12	1.2
HGF	1.3
TGF- α	1.4
IL-6	2.0
IFN- γ	2.4
TNF- α	3.3
VEGF	3.7
IL-1 β	12.0
MMP-9	0.4
MMP-2	0.6
MMP-7	1.9
MMP-1b	2.9
MMP-3	2.9
MMP-13	2.9
MMP-1a	3.6
MMP-16	4.1
MMP-10	11.6

doi:10.1371/journal.pone.0089605.t001

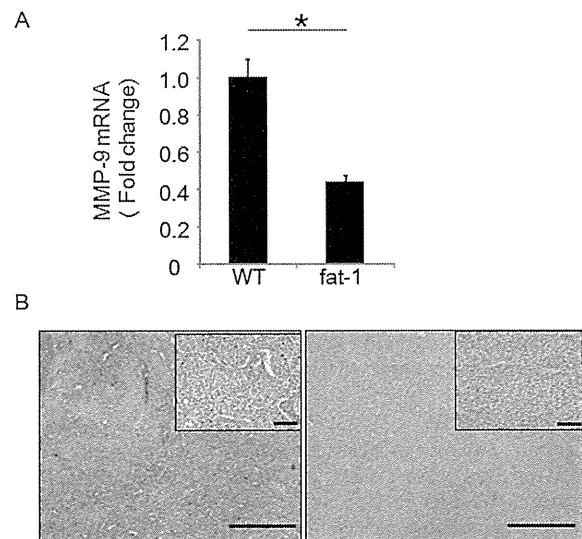


Figure 3. MMP-9 expression is downregulated in TC-1 tumors from fat-1 mice. Total RNA was extracted from TC-1 tumors, followed by reverse transcription. MMP-9 mRNA levels were measured by qRT-PCR. Expression levels of MMP-9 were normalized to β -actin as an internal standard (n=4 in each group). Asterisks indicate those comparisons (fat-1 vs. wild type (WT) mice) with statistical significance ($p<0.05$). MMP-9 immunostaining of TC-1 tumors derived from wild type (WT) and fat-1 mice. Bars indicate 200 μ m in low-power fields, 50 μ m in high-power fields. doi:10.1371/journal.pone.0089605.g003

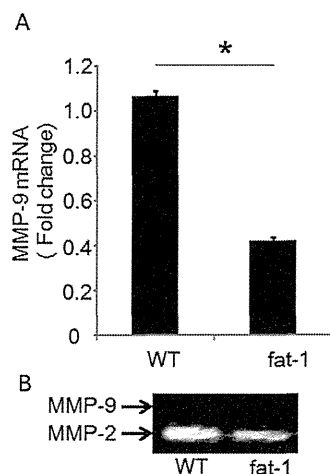


Figure 4. MMP-9 expression and enzymatic activity in primary-cultured fibroblasts. (A) Primary fibroblasts isolated from murine lungs were cultured. Total RNA from fibroblasts was reverse transcribed and MMP-9 mRNA levels were measured by qRT-PCR. Expression levels of MMP-9 were normalized to β -actin as an internal standard. Data are the representative of three independent experiments. The data were analyzed by using the Student's *t*-test. Asterisks indicate those comparisons (fat-1 vs. wild type (WT) mice) with statistical significance ($p < 0.05$). (B) Gelatin zymography: Supernatant from primary fibroblast cultures were collected and separated by electrophoresis. Gelatinase activities were visualized by standard staining techniques. doi:10.1371/journal.pone.0089605.g004

supernatants from each primary fibroblast subtype were collected and subjected to polyacrylamide gel electrophoresis to examine differences in MMP gelatinase activities (Fig. 4B). Using this method, MMP-2 was detected but MMP-9 was not in both fat-1 and wild type fibroblast

Next, these primary fibroblasts were co-cultured with TC-1 cells to examine fibroblasts activation upon in vitro exposure to cancer cells¹¹. Fibroblasts and TC-1 cells were co-cultured for 24 hours and MMP-9 transcription was measured by RT-qPCR. Fibroblasts from fat-1 and from wild type mice increased demonstrated MMP-9 expression upon exposure to TC-1 cells (Fig. 5A). In fibroblasts derived from fat-1 mice, the extent of MMP-9 induction was lower than that in fibroblasts from wild type mice (Fig. 5A). MMP-9 was not expressed in homotypic TC-1 cells, consistent with immunohistochemical data from our in vivo model. Furthermore, we confirmed that MMP-9 was not expressed in the TC-1 cells by using a transwell co-culture model (Fig. S2). Therefore, MMP-9 in the co-culture condition was derived not from TC-1 cells but from fibroblasts. MMP-2 gelatinase activity was detected in all cell culture conditions, including homotypic TC-1 cell cultures, and was not altered by co-culture conditions (Fig 5B, 5D). MMP-9 gelatinase activities were, however, detectable in fibroblast-TC-1 cell co-cultures, although MMP-9 gelatinase activity involving fat-1 fibroblasts was clearly suppressed when compared with wild type fibroblasts (Fig 5B, 5C), again supporting the concept that MMP-9 expression and gelatinase activity are suppressed by endogenous omega-3 PUFAs in CAFs derived from fat-1 mice.

Discussion

In this study, we examined the involvement of defined dietary factors (omega-3 and omega-6 PUFAs) in tumorigenesis using

HPV-positive TC-1 cells and proposed a novel anti-tumor mechanism for omega-3 PUFAs that depends on the activities of CAFs. Omega-3 PUFAs have been shown to suppress cancer incidence and growth in various types of cancers [18,19,27]. Many studies have demonstrated that omega-3 PUFAs have these effects through anti-inflammatory responses directly and/or indirectly [25–27] as well as through inducing tumor cell apoptosis and/or suppressing tumor cell proliferation [18,19]. However, there have been few reports about the effects of omega-3 PUFAs on CAFs. CAFs have been implicated in facilitating the growth of several tumors by directly stimulating tumor cell proliferation and by enhancing angiogenesis [34,35]. Targeting genes and signaling pathways mediating interaction of CAFs and tumor-microenvironment are considered to be essential for development of new and effective cancer therapies [36,37]. In this study, using fat-1 mice and TC-1 tumor cells, we were able to clarify the effect of omega-3 PUFA-rich CAFs on tumorigenesis.

Many molecules, including growth factors, cytokines, and MMPs, play stimulatory and inhibitory roles in promoting angiogenesis [21]. We investigated gene expression of angiogenesis-related cytokines, growth factors and MMPs in the TC-1 tumors of fat-1 and wild type mice by cDNA microarray. The expression levels of almost all inflammatory cytokines/chemokines and growth factors in TC-1 tumors from fat-1 mice were higher than those in tumors from wild-type controls. In contrast, EGF and MMP-2 and -9 expression levels in fat-1 mice were lower than those in wild type mice. Since down-regulation of EGF in TC-1 tumors from fat-1 mice was predicted to promote TC-1 cell proliferation but tumor size in fat-1 mice was significantly smaller than in wild-type controls, we hypothesize that differences in MMP production between fat-1 and wild type mice may be responsible for the suppression of TC-1 tumor growth. Our in vitro data verified that MMP-9 derived from CAFs activated by TC-1 cell exposure was downregulated in the fat-1 mice. MMPs are reported to influence tumor progression by facilitating events pivotal for neovascularization and for the establishment of distant metastasis including proliferation, survival and migration of endothelial, tumor and stromal cells [8,9]. MMP inhibitors reduce angiogenesis, tumor number, and tumor growth, as does genetic ablation of MMP-9 [38]. In contrast to MMP-2, which is constitutively expressed, MMP-9 levels are usually low and enzyme expression is induced by cytokines that stimulate NF- κ B [8,39]. Furthermore, elevated serum and tissue levels of MMP-9 are reported to be associated with cancer invasion and metastasis [40]. In breast cancer, MMP-9 activity has been localized around CAFs and CAFs co-cultured with cancer cells which secrete TGF- β , TNF- α , and other cytokines, increase production of MMP-9 [11], consistent with our in vitro data. In our data, suppression of MMP-9 would contribute to accompany hypo-angiogenesis in the tumor stromal component in fat-1 tumor.

Several transcription factors, including activator protein-1 (AP-1), Sp-1, and NF- κ B, are reported to be involved in alterations in MMP-9 expression following exposure to various cytokines [41–43]. Conversely, several reports have demonstrated that omega-3 PUFAs have an inhibitory effect on the NF- κ B pathway when activated by various stimuli [43–47]. Our own data suggest that activation of the NF- κ B pathway upon co-culture with TC-1 cells may be suppressed by elevated level of omega-3 PUFAs in fibroblast obtained from fat-1 mice.

In our experiments, we consistently used primary fibroblasts that had been passaged 3–4 times only. Nevertheless, lipid mediator analysis of the fibroblasts revealed that those derived from fat-1 mice produced larger amounts of omega-3 PUFAs including EPA-derived metabolites when compared with those

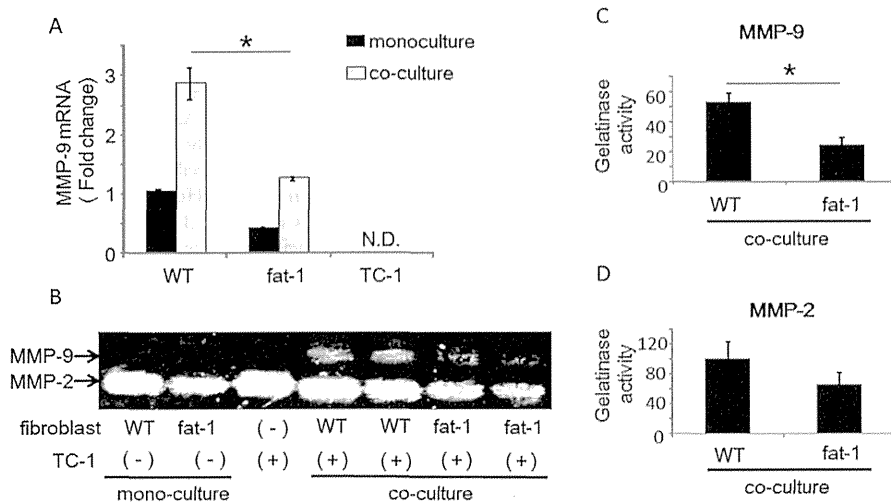


Figure 5. The increased MMP-9 expression and activity in TC-1/fibroblast co-cultures is inhibited in fat-1 mice. (A) Isolated fibroblasts were co-cultured with TC-1 cells for 24 hours and expression levels of MMP-9 in the fibroblasts were measured by RT-qPCR. Expression levels of MMP-9 were normalized to β -actin as an internal standard. The data are representative of three independent experiments. The data were analyzed using the Student's *t*-test. Asterisks indicate those comparisons (fat-1 vs. wild type (WT) mice) with statistical significance ($p < 0.05$). "N.D." indicates 'not detected'. (B) Gelatin zymography: Supernatants from fibroblast homotypic cultures and fibroblast/TC-1 co-cultures were collected and separated by electrophoresis. Gelatinase activities were visualized by standard staining techniques. (C, D) For semi-quantitative analyses, gelatin zymography bands were analyzed using image analysis software. Results are represented as mean \pm SEM of three independent experiments. The data were analyzed using the Student's *t*-test. Asterisks indicate those comparisons (fat-1 vs. wild type (WT) mice) with statistical significance ($p < 0.05$). doi:10.1371/journal.pone.0089605.g005

derived from wild type controls (Fig.S3), confirming that the cultured fibroblasts retained the characteristic to make omega-3 PUFA rich environment.

TC-1 tumor microarray data showed that several inflammatory cytokines/chemokines and growth factors were upregulated in fat-1 mice. However, the data indicated gene expression levels in both TC-1 cells and stromal components, including fibroblasts, endothelial and immune cells. Therefore, expression levels of each cytokine/chemokine were dependent on their primary sources of production. MMP-9 was produced by the fibroblasts derived from fat-1 mice but not by TC-1 cells. Therefore, suppression of the NF- κ B pathway by elevated levels of omega-3 PUFAs in fat-1-derived stromal components may have a specific and potent effect on MMP-9 expression levels when compared with the other inflammatory cytokines/chemokines. On the other hand, a previous study demonstrates that omega-3 PUFAs activate NK cells and increase proportions of activated CD8⁺ cells; this is followed by enhanced anti-tumor effects [48]. Therefore, omega-3 PUFAs may exert both anti-inflammatory and pro-inflammatory effects on immune cells.

In this study, we have demonstrated that an omega-3 PUFAs-rich microenvironment can suppress MMP-9 secretion from CAFs and that this is associated with subsequent tumor hypo-angiogenesis. This study proposes a novel anti-tumor effect of omega-3 PUFAs by modulating tumor microenvironment especially on CAFs.

Supporting Information

Figure S1 Expression levels of E6 and E7 mRNA in TC-1 tumor. Total RNA was extracted from TC-1 tumors, followed by reverse transcription. E6 and E7 mRNA levels were measured by qRT-PCR. Expression levels of E6 and E7 mRNA were normalized to β -actin as an internal standard. The E6 primers were forward, 5'- TGCACAGAGCTGCAAACAAC -3', and

reverse, 5'- AGCATATGGATTCCCATCTC -3'. The E7 primers were forward, 5'- TTTGCAACCAGAGACAACTGA -3', and reverse, 5'- GCCCATTAACAGGTCTTCCA -3'.

(TIF)

Figure S2 MMP-9 mRNA was not induced from TC-1 cells by co-culture with fibroblasts. 150 μ L of suspensions (2×10^6 /mL) of TC-1 cells or fibroblasts were added to the upper chamber, 500 μ L of suspensions (1×10^5 /mL) of TC-1 cells or fibroblasts were added to the lower chamber of the 24 well Transwell plates (1 μ m pore) and placed in an incubator with 5% CO₂ at 37°C for 24 h and expression levels of MMP-9 in the TC-1 or fibroblasts in the lower chamber were measured by RT-qPCR. N.D. indicates 'not detected'.

(TIF)

Figure S3 Lipid mediator analysis of fibroblast/TC-1 co-cultured medium. Supernatants from fibroblast/TC-1 co-cultures were collected and LC-MS/MS-based mediator lipidomics was performed on Acquity UPLC BEH C₁₈ column (1.0 mm \times 150 mm \times 1.7 μ m) using Acquity UltraPerformance LC system (Waters Co.) coupled to an electrospray (ESI) triple quadrupole mass spectrometer (QTRAP5500; AB SCIEX). The MS/MS analyses were performed in negative ion mode, and the eicosanoids and docosanoids were identified and quantified by multiple reaction monitoring. Calibration curves between 1 and 1000 pg and the LC retention times for each compounds were constructed with synthetic standards.

(TIF)

Acknowledgments

We gratefully thank Dr. Danny J. Schust for careful editing of the manuscript and Dr. Terufumi Yokoyama for excellent comments and advice on experiments using murine models.

Author Contributions

Conceived and designed the experiments: AT K. Kawana KT AY MA K. Koga. Performed the experiments: AT K. Kawana KT AY YI KN TI HN

References

- Lorusso G, Ruegg C (2008) The tumor microenvironment and its contribution to tumor evolution toward metastasis, *Histochem Cell Biol*, 130:1091–1103
- Joyce JA, Pollard JW (2009) Microenvironmental regulation of metastasis, *Nat Rev Cancer*, 9:239–252
- Franco OE, Shaw AK, Strand DW, Hayward SW (2010) Cancer associated fibroblasts in cancer pathogenesis, *Semin Cell Dev Biol*, 21:33–39
- Kalluri R, Zeisberg M (2006) Fibroblasts in cancer, *Nat Rev Cancer*, 6:592–401
- Schauer IG, Zhang J, Xing Z, Guo X, Mercado-Urbe I, et al (2013) Interleukin-1 β promotes ovarian tumorigenesis through a p53/NF-kappaB-mediated inflammatory response in stromal fibroblasts, *Neoplasia*, 15:409–420
- Zhu Y, Zhu M, Lance P (2012) IL1 β -mediated Stromal COX-2 signaling mediates proliferation and invasiveness of colonic epithelial cancer cells, *Exp Cell Res*, 318:2520–2530
- Jones CB, Sane DC, Herrington DM (2003) Matrix metalloproteinases, *Cardiovas Res*, 59:812–823
- Lynch CC, Matrisian LM (2002) Matrix metalloproteinases in tumor-host cell communication, *Differentiation*, 70:561–573
- Chantrain CF, Shimada H, Jodele S, Groshen S, Ye W, et al (2004) Stromal Matrix Metalloproteinase-9 Regulates the Vascular Architecture in Neuroblastoma by Promoting Pericyte Recruitment, *Cancer Res*, 64:1675–1686
- Roomi MW, Monterrey JC, Kalinsky T, Niedzwiecki A, Rath M (2009) Modulation of MMP-2 and MMP-9 by cytokines, mitogens and inhibitors in lung cancer and malignant mesothelioma cell lines, *Oncol Rep*, 22:1283–1291
- Suelten CH, Byfield SD, Arany PR, Karpova TS, Stetler-Stevenson WG, et al (2005) Breast cancer cells induce stromal fibroblasts to express MMP-9 via secretion of TNF- α and TGF- β , *Journal of Cell Sci*, 118:2143–2153
- Genersch E, Hayess K, Neuenfeld Y, Haller H (2000) Sustained ERK phosphorylation is necessary but not sufficient for MMP-9 regulation in endothelial cells: involvement of Ras-dependent and -independent pathways, *J Cell Sci*, 113 Pt 23:4319–4330
- Heissig B, Hattori K, Friedrich M, Rafii S, Werb Z (2003) Angiogenesis: vascular remodeling of the extracellular matrix involves metalloproteinases, *Current Opinion in Hematol*, 10:136–141
- Serhan CN, Savill J (2005) Resolution of inflammation: the beginning programs the end, *Nat Immunol*, 6:1191–1197
- Hardman WE (2002) Omega-3 fatty acids to augment cancer therapy, *J Nutr*, 132:350S–351S
- Lee CY, Sit WH, Fan ST, Man K, Jor IW, et al (2010) The cell cycle effects of docosahexaenoic acid on human metastatic hepatocellular carcinoma proliferation, *Int J Oncol*, 36:991–998
- Habermann N, Schon A, Lund EK, Gleit M (2010) Fish fatty acids alter markers of apoptosis in colorectal adenoma and adenocarcinoma cell lines but fish consumption has no impact on apoptosis-induction ex vivo, *Apoptosis*, 15:621–630
- Serini S, Piccioni E, Merendino N, Calviello G (2009) Dietary polyunsaturated fatty acids as inducers of apoptosis: implications for cancer, *Apoptosis*, 14:135–152
- Field CJ, Schley PD (2004) Evidence for potential mechanisms for the effect of conjugated linoleic acid on tumor metabolism and immune function: lessons from n-3 fatty acids, *Am J Clin Nutr*, 79:1190S–1198S
- Calviello G, Di Nicuolo F, Gragnoli S, Piccioni E, Serini S, et al (2004) n-3 PUFAs reduce VEGF expression in human colon cancer cells modulating the COX-2/PGE2 induced ERK-1 and -2 and HIF-1 α induction pathway, *Carcinogenesis*, 25:2303–2310
- Spencer L, Mann C, Metcalfe M, Webb MB, Pollard C, et al (2009) The effect of omega-3 FAs on tumour angiogenesis and their therapeutic potential, *Eur J cancer*, 45:2077–2086
- Rose DP, Connolly JM (1999) Antiangiogenicity of docosahexaenoic acid and its role in the suppression of breast cancer cell growth in nude mice, *Int J Oncol*, 15:1011–1015
- Mukutmoni-Norris M, Hubbard NE, Erickson KL (2000) Modulation of murine mammary tumor vasculature by dietary n-3 fatty acids in fish oil, *Cancer Lett*, 150:101–109
- Tevaz R, Jho DH, Babcock T, Helton WS, Espat NJ (2002) Omega-3 fatty acid supplementation reduces tumor growth and vascular endothelial growth factor expression in a model of progressive non-metastasizing malignancy, *JPEN J Parenter Enteral Nutr*, 26:285–289
- Kang JX (2007) Fat-1 transgenic mice: a new model for omega-3 research, *Prostaglandins Leukot Essent Fatty Acids*, 77:263–267
- Kang JX, Wang J, Wu L, Kang ZB (2004) Transgenic mice: fat-1 mice convert n-6 to n-3 fatty acids, *Nature*, 427:504
- Xia S, Lu Y, Wang J, He C, Hong S, et al (2006) Melanoma growth is reduced in fat-1 transgenic mice: Impact of omega-6/omega-3 essential fatty acids, *PNAS*, 103:12499–12504
- Nowak J, Weylandt KH, Habbal P, Wang J, Dignass A, et al (2007) Colitis-associated colon tumorigenesis is suppressed in transgenic mice rich in endogenous n-3 fatty acids, *Carcinogenesis*, 28:1991–1995
- Jia Q, Lupton JR, Smith R, Weeks BR, Callaway E, et al (2008) Reduced Colitis-Associated Colon Cancer in Fat-1 (n-3 Fatty Acid Desaturase) Transgenic Mice, *Cancer Res*, 68:3985–3991
- Weylandt KH, Krause LF, Gomolka B, Chiu C-Y, Bilal S, et al (2011) Suppressed liver tumorigenesis in fat-1 mice with elevated omega-3 fatty acids is associated with increased omega-3 derived lipid mediators and reduced TNF- α , *Carcinogenesis*, 32:897–903
- zur Hausen H (2009) Papillomaviruses in the causation of human cancers — a brief historical account, *Virology*, 384:260–265
- Lin KY, Guarnieri FG, Staveley-O'Carroll KF, Levitsky HI, August JT, et al (1996) Treatment of established tumors with a novel vaccine that enhances major histocompatibility class II presentation of tumor antigen, *Cancer Res*, 56:21–26
- Rowe RG, Keena D, Sabeh F, Willis AL, Weiss SJ (2011) Pulmonary fibroblasts mobilize the membrane-tethered matrix metalloprotease, MT1-MMP, to destructively remodel and invade interstitial type I collagen barriers, *Am J Physiol Lung Cell Mol Physiol*, 301:L683–692
- Erez N, Truitt M, Olson P, Arron ST, Hanahan D (2010) Cancer-Associated Fibroblasts Are Activated in Incipient Neoplasia to Orchestrate Tumor-Promoting Inflammation in an NF-kappaB-Dependent Manner, *Cancer Cell*, 17:135–147
- Bhowmick NA, Neilson EG, Moses HL (2004) Stromal fibroblasts in cancer initiation and progression, *Nature*, 432:332–337
- Hanahan D, Coussens LM (2012) Accessories to the crime: functions of cells recruited to the tumor microenvironment, *Cancer Cell*, 21:309–322
- Valastyan S, Weinberg RA (2011) Tumor metastasis: molecular insights and evolving paradigms, *Cell*, 147:275–292
- Bergers G, Brekken R, McMahon G, Vu TH, Itoh T, et al (2000) Matrix metalloproteinase-9 triggers the angiogenic switch during carcinogenesis, *Nat Cell Biol*, 2:737–744
- Sternlicht MD, Werb Z (2001) How matrix metalloproteinases regulate cell behavior, *Annu Rev Cell Dev Biol*, 17:463–516
- Nabeshima K, Inoue T, Shimao Y, Sameshima T (2002) Matrix metalloproteinases in tumor invasion: role for cell migration, *Pathol Int*, 52:255–264
- Kupferman ME, Fini ME, Muller WJ, Weber R, Cheng Y, et al (2000) Matrix metalloproteinase 9 promoter activity is induced coincident with invasion during tumor progression, *Am J Pathol*, 157:1777–1783
- Simon C, Simon M, Vucelic G, Hicks MJ, Plinkert PK, et al (2001) The p38 SAPK pathway regulates the expression of the MMP-9 collagenase via AP-1-dependent promoter activation, *Exp Cell Res*, 271:344–355
- Kim HH, Lee Y, Eun HC, Chung JH (2008) Eicosapentaenoic acid inhibits TNF-alpha-induced matrix metalloproteinase-9 expression in human keratinocytes, HaCaT cells, *Biochem Biophys Res Commun*, 368:343–349
- Mishra A, Chaudhary A, Sethi S (2004) Oxidized omega-3 fatty acids inhibit NF-kappaB activation via a PPARalpha-dependent pathway, *Arterioscler Thromb Vasc Biol*, 24:1621–1627
- Dichtl W, Ares MP, Jonson AN, Jovine S, Pachinger O, et al (2002) Linoleic acid-stimulated vascular adhesion molecule-1 expression in endothelial cells depends on nuclear factor-kappaB activation, *Metabolism*, 51:327–333
- Zhao Y, Joshi-Barve S, Barve S, Chen LH (2004) Eicosapentaenoic acid prevents LPS-induced TNF-alpha expression by preventing NF-kappaB activation, *J Am Coll Nutr*, 23:71–78
- Ross JA, Maingay JP, Fearon KC, Sangster K, Powell JJ (2003) Eicosapentaenoic acid perturbs signalling via the NFkappaB transcriptional pathway in pancreatic tumour cells, *Int J Oncol*, 23:1733–1738
- Robinson LE, Clandinin MT, Field CJ (2002) The role of dietary long-chain n-3 fatty acids in anti-cancer immune defense and R3230AC mammary tumor growth in rats: influence of diet fat composition, *Breast Cancer Res Treat*, 73:145–160

Resveratrol suppresses inflammatory responses in endometrial stromal cells derived from endometriosis: A possible role of the sirtuin 1 pathway

Ayumi Taguchi, Osamu Wada-Hiraike, Kei Kawana, Kaori Koga, Aki Yamashita, Akira Shirane, Yoko Urata, Shiro Kozuma, Yutaka Osuga and Tomoyuki Fujii

Department of Obstetrics and Gynecology, Faculty of Medicine, The University of Tokyo, Tokyo, Japan

Abstract

Aim: Endometriosis is a chronic inflammatory disease. Sirtuin 1 (SIRT1) plays a role in regulation of inflammation. The role of SIRT1 in endometriosis remains unknown. We here addressed the anti-inflammatory effects of SIRT1 on endometriosis.

Methods: The expression of SIRT1 in human ovarian endometriomas and eutopic endometria were examined using immunohistochemistry and reverse transcription polymerase chain reaction (RT-PCR). Endometriotic stromal cells (ESC) obtained from endometriomas were exposed to either resveratrol or sirtinol, an activator or inhibitor of sirtuins, respectively, and tumor necrosis factor (TNF)- α -induced interleukin (IL)-8 release from the ESC was assessed at mRNA and protein levels.

Results: Both immunohistochemistry and RT-PCR demonstrated that SIRT1 was expressed in ESC and normal endometrial stromal cells. Resveratrol suppressed TNF- α -induced IL-8 release from the ESC in a dose-dependent manner while sirtinol increased IL-8 release.

Conclusion: These opposing effects of SIRT1-related agents suggest that IL-8 release from the ESC is modulated through the SIRT1 pathway. Resveratrol may have the potential to ameliorate local inflammation in endometriomas.

Key words: endometriosis, inflammation, interleukin-8, resveratrol, sirtinol, tumor necrosis factor- α .

Introduction

Endometriosis, defined as the presence of endometrial tissue outside of the uterus, represents a common gynecological condition that tends to be associated with pelvic pain and infertility.¹ Inflammation plays an important role in the development of endometriosis.^{2–4} Some studies have demonstrated that cytokines in the peritoneal fluid of endometriosis patients contribute to the establishment and proliferation of ectopic endometrial implants.⁵ More specifically, the peritoneal fluid

from patients with endometriosis has been shown to possess elevated levels of pro-inflammatory cytokines derived from the lesions themselves, from activated macrophages and from other immune cells.^{1,6}

These cytokines are under the control of nuclear factor (NF)- κ B, a central regulator of immune system gene expression. NF- κ B is an important transcription factor in inflammatory and other immune pathways and the activation of NF- κ B plays a critical role in the progression of endometriosis. NF- κ B can be activated by pro-inflammatory cytokines like tumor necrosis

Received: May 1 2013.

Accepted: July 27 2013.

Reprint request to: Dr Kei Kawana, Department of Obstetrics and Gynecology, Graduate School of Medicine, The University of Tokyo, 7-3-1 Hongo, Bunkyo-ku, Tokyo 113-8655, Japan. Email: kkawana-ky@umin.org

Conflict of interest: None of the authors have any financial support or relationships that may pose a conflict of interest related to this study.